Motor and sensitive recovery after injection of a physically cross-linked PNIPAAm-g-PEG hydrogel in rat hemisectioned spinal cord

Maxime Bonnet, Thomas Trimaille, Jean-Michel Brezun, François Feron, Didier Gigmes, Tanguy Marqueste, Patrick Decherchi

Materials Science & Engineering C 107 (2020) 110354

Contents lists available at ScienceDirect

Materials Science & Engineering C

journal homepage: www.elsevier.com/locate/msec

Motor and sensitive recovery after injection of a physically cross-linked PNIPAAm-*g*-PEG hydrogel in rat hemisectioned spinal cord

Maxime Bonnet[a], Thomas Trimaille[b], Jean-Michel Brezun[a], François Feron[c], Didier Gigmes[b], Tanguy Marqueste[a,1], Patrick Decherchi[a,*,1]

[a] Aix Marseille Univ, CNRS, ISM, UMR 7287 « Institut des Sciences du Mouvement: Etienne-Jules MAREY », Equipe « Plasticité des Systèmes Nerveux et Musculaire » (PSNM), Parc Scientifique et Technologique de Luminy, Faculté des Sciences du Sport de Marseille, CC910 - 163 Avenue de Luminy, F-13288, Marseille, Cedex 09, France
[b] Aix Marseille Univ, CNRS, ICR, UMR 7273 « Institut de Chimie Radicalaire », Equipe « Chimie Radicalaire Organique et Polymères de Spécialité » (CROPS), Case 562 - Avenue Escadrille Normandie-Niemen, F-13397, Marseille, Cedex 20, France
[c] Aix Marseille Univ, CNRS, INP, UMR 7051 « Institut de Neuropathophysiologie », Equipe « Gènes, Rythmes et Neuropathophysiologie » (GRN), 51, boulevard Pierre Dramard - CS80011, F-13344, Marseille, Cedex 15, France

ARTICLE INFO

Keywords:
Lesion
Biomaterial
Reflex
Inflammation
Sensorimotor loop

ABSTRACT

In line with experiments showing that implanted hydrogels are promising tools, we designed and injected, after a C2 spinal cord hemisection, a thermoresponsive and thermoreversible physically cross-linked poly(N-isopropylacrylamide)-poly(ethylene glycol) copolymer in order to reduce functional deficits and provide a favorable environment to axotomized axons.

Nasal olfactory ecto-mesenchymal stem cells were cultured on the hydrogel in order to verify its biocompatibility. Then, inflammatory reaction (Interleukin-1β and 6, Tumor Necrosis Factor-α) was examined 15 days post-hydrogel injection. Functional recovery (postural and locomotor activities, muscle strength and tactile sensitivity) was assessed once a week, during 12 weeks. Finally, at 12 weeks post-injection, spinal reflexivity and ventilatory adjustments were measured, and the presence of glial cells and regenerated axons were determined in the injured area.

Our results indicate that cells survived and proliferated on the hydrogel which, itself, did not induce an enhanced inflammation. Furthermore, we observed significant motor and sensitive improvements in hydrogel-injected animals. Hydrogel also induced H-reflex recovery close to control animals but no improved ventilatory adjustment to electrically-evoked isometric contractions. Finally, regrowing axons were visualized within the hydrogel with no glial cells colonization.

Our results emphasize the effectiveness of our copolymer and its high therapeutic potential to repair the spinal cord after injury.

1. Introduction

In animal models of spinal cord injury (SCI), the implantation of biomaterials seems to be a promising strategy allowing to reduce inflammatory reaction and glial scar formation, and to promote axonal regeneration and functional recovery. These biomaterials can be natural (i.e., biopolymers of agarose, alginate, chitosan, collagen, fibrin …), synthetic [poly(2-hydroxyethyl methacrylate) (pHEMA), poly (lactic acid) (PLA), polyethylene glycol (PEG), poly(D,L-lactic acid-co-glycolic acid) (PLGA) ….] or hybrid (hyaluronic acid-PEG, chitosan-methacrylamide, …), cytocompatible, non-immunogenic, chemically stable, degradable and resorbable [1–9]. They have been used for delivering drug and cells, limiting the inflammatory reaction and the glial scar development, filling the cystic cavities and/or providing structural support for regenerating neurons after a SCI [10,11]. However, natural and hybrid materials have some disadvantages like, among others, the risk of disease transmission and the ability to provoke an immune response [12].

Synthetic homopolymeric, co-polymeric and semi-/inter-penetrating polymer network hydrogels are attractive biomaterials to repair the brain after a traumatic injury and bridge a cavity, after a SCI or a peripheral nerve lesion [13–15]. They can be nontoxic and chemically

* Corresponding author. Aix Marseille Univ, CNRS, ISM, CC910 - 163, avenue de Luminy, F-13288, Marseille, Cedex 09, France.
E-mail address: patrick.decherchi@univ-amu.fr (P. Decherchi).
URL: https://ism.univ-amu.fr (P. Decherchi).
[1] Equally supervising authors.

https://doi.org/10.1016/j.msec.2019.110354
Received 19 April 2019; Received in revised form 2 October 2019; Accepted 20 October 2019
Available online 23 October 2019

inert. Furthermore, these polymers display other advantages. They are composed of macromolecular networks of cross-linked hydrophilic molecules or polymers, readily saturated with water, that mimic the extracellular matrix (ECM) [9]. Being a 3D porous construction with interconnected pores, they can act as a scaffold and allow cell migration and nutriment diffusion as well as neovascularization of the implant [7,16,17]. Contrary to natural hydrogels, they are more amenable to modification (i.e., protein adsorption and cellular interaction depend of the degree of hydrophilicity), easily reproduced and free of residual growth factors and undefined and/or non-quantified constituents [18]. Thus, some of these synthetic hydrogels (co-polypeptide, poly-alkylimide, hydroxy ethyl methacrylate [2-(methacryloyloxy)ethyl] trimethylammonium chloride (HEMA-MOETACl), poly(vinyl acetate) (PVA)) have been proven to be biocompatible [19–23]. Others like PEG, pHEMA, poly N-(2-hydroxypropyl)-methacrylamide (pHPMA) and poly (2-hydroxyethyl methacrylate-co-methyl methacrylate) (PHEMA-MMA), polyethylene glycol-poly-L-lysine (PEG-PLL) are able to reduce the glial scar formation and/or to provide a cellular framework for regenerating tissue in the injured spinal cord [14,24–40]. Among these synthetic hydrogels, acrylamide and methacrylamide polymers, as acrylate and methacrylate polymers, with similar mechanical properties for the spinal cord [41], are suitable implantation materials that can i) prevent the development of the glial scar and necrotic tissue and ii) promote axonal regeneration and behavioral recovery [25,26,36,42].

In addition to these conventional hydrogels, “smart or intelligent” hydrogels, responding for example to stimuli like pH, light radiation, temperature, magnetic and electric field, ionic concentration, ultrasound were devised [43]. These stimuli-responsive hydrogels are of great interest for complex SCI, displaying irregular and/or multi-shape cavities (i.e., little void spaces and high tortuosities). Thus, *in situ* forming hydrogels, be easily shaped or injected to fill the entire lesion cavity offer a minimally invasive delivery compared to implanted hydrogels [44]. Indeed, hydrogel injected through a fine needle is less invasive than physical implant and thereby facilitates surgery and recovery. In this context, self-assembling nanofibers, that spontaneously aggregate from an aqueous solution into a stable gel in the presence of a physiological salt solution or when the pH changes, were able to inhibit glial scar formation and promote axon elongation after SCI [45]. Similarly, synthetic self-assembling peptide amphiphile hydrogels, liquid at ambient temperature and organized in nanofibers after injection in the lesion cavity, reduce astrogliosis and cell death, while enhancing axonal regeneration, when injected in injured spinal cord [19,46,47]. PLA-PEG-PLA triblock copolymer polymerized *in situ* using a photoinitiator and light was used for delivery of NT-3 to the injured spinal cord in rats [48].

Thermoresponsive hydrogels have the particularity to turn from solution to gel when the temperature changes without any additional external factor [49]. Hydrogels displaying a suitable low critical solution temperature (LCST) (i.e; a gelling behavior when the temperature increases and reaches the body temperature) were intensively studied but few were proposed for spinal cord repair. Among the main synthetic hydrogels with thermosensitive sol-gel transition behavior and their copolymers, poly(ethylene oxide)-*b*-poly(propylene oxide)-*b*-poly (ethylene oxide) (PEO-PPO-PEO) triblock copolymer also, named Pluronics®-F127 (poloxamer 407), was used for localized drug delivery and cell encapsulation [50–56]. Oligo(ethylene glycol) methacrylate (OEGMA) monomers have also been proposed for localized drug delivery [57]. Copolypeptide hydrogels containing poly(L-leucine), L, or poly(γ-[2-(2-methoxyethoxy)ethyl]-L-glutamate-*stat*-L-leucine), (EP2/L) and poly(γ-[2-(2-methoxyethoxy)ethyl]-*rac*-glutamate) were also considered for *in vivo* cell and molecule delivery [58]. Chen et al. reported that injectable PLGA-PEG-PLGA triblock copolymer hydrogel, containing or not dexamethasone, prevents epidural scar formation after laminectomy [59]. More recently, it was reported that injection of poly (organophosphazenes) into spinal cord contusion-provoked cavities induce bridging effects with beneficial ECM remodeling and regeneration of 5-HT axons, probably contributing to the recovery of locomotor function, when combined to imidazole [60,61].

Poly(N-isopropylacrylamide) (PNIPAAm) and its copolymers are thermoresponsive and thermoreversible hydrogels [62] that express reversible swelling and shrinking behaviors when the temperature fluctuates, without the use of toxic monomers or cross-linkers [63–65]. These semi-porous gels allow cell attachment, growth and spread in certain conditions [66,67]. They were used for drug delivery, cell encapsulation and delivery and cell culture surfaces [68–74]. NIPAAm has a LCST around 32 °C in pure water and, when copolymerized with a more hydrophilic polymer, the LCST increases inside of the physiological temperature range (i.e., 37 °C). Furthermore, when combined to PEG, the mechanical and swelling properties of the polymer can be tailored [63].

PEG is a biocompatible and non-toxic biodegradable synthetic material that inhibits the inflammatory response following SCI, provides neuroprotection (i.e., protects cell integrity and mitochondria, reduces cell apoptosis, inhibits free radicals, prevents lipid peroxidation, …), reduces microenvironment changes (glial scar and vacuoles formation, cell aggregation, ….) and plays a role in nerve fiber regeneration [37]. However, it was suggested that PEG alone has several shortcomings and the efficacy of PEG is not ideal. Indeed, PEG alone is an implantable hydrogel that cannot fully fill the lesion cavity and mimic the 3D porous structure of the spinal cord.

Finally, when NIPAAm is copolymerized with hydrophilic macromers of methacrylated PEG, the syneresis of its hydrophobic chains is minimized above the LCST, and its elastic property and porosity are increased [63,75]. Furthermore, *in vitro* and at physiological temperature, its volume retention in Dulbecco's Modified Eagle's medium (DMEM) with Nutrient Mixture F-12 with serum of PBS was around 100%, making it suitable for tissue engineering implants [76]. Finally, by introducing a PEG block that changes the physicochemical properties of the copolymer, it becomes more biocompatible than Poloxamers [75].

Thus, PNIPAAm-*g*-PEG combined to arginyl-glycyl-α-aspartyl-serinyl (RGDS) peptide was used as cell culture material [77]. Furthermore, in order to repair a partial spinal cord injury, PNIPAAm-*g*-PEG was combined to BDNF or NT-3 [76,78,79]. The authors demonstrated that PNIPAAm-*g*-PEG hydrogel i) was biocompatible with mesenchymal stem cells, ii) matched to the mechanical properties of the neuronal tissue (i.e., compressive modulus between 3 and 5 kPa) and sustained a drug release for up to 4 weeks. They showed that hydrogel was an effective vehicle for delivery of skin fibroblast transplants and was permissive to axonal growth. However, although the authors compared the PNIPAAm-*g*-PEG hydrogel to commercially available collagen-based matrices such as Gelfoam® and Vitrogen/PureCol®, they did not compare their results to SCI animals without hydrogel injection. Furthermore, the PNIPAAm-*g*-PEG hydrogel used in these studies was chemically cross-linked (use of PEG-dimethacrylate), raising the problem of impossible renal clearance and long-term tissue accumulation.

In the current study, before evaluating the *in vivo* functional performance of a PNIPAAm-*g*-PEG hydrogel on a rodent model of cervical spinal cord hemisection, the biocompatibility of the hydrogel was first evaluated as a substrate for cultivated cells. Further, a cell-free hydrogel was injected as viscous liquid into the lesion cavity, before formed a semi-solid space-filling matrix. The host immune response to the hydrogel was evaluated, at Week 2 post-injection, by measuring the level of tumor necrosis factor (TNF)-α and interleukin (IL)-1β and 6, with an Elisa assay. Furthermore, sensory and motor recovery in the anterior and posterior legs was weekly assessed, during 3 months, using 4 behavioral tests. Then, at Month 3, spinal reflexivity and physiological adjustments to muscle fatigue were evaluated. Finally, the spinal cords were collected for assessing of the presence of the hydrogel within the lesion cavity and axonal growth. All injected animals were compared to lesioned animals without gel insertion.

2. Materials and methods

2.1. Animals

Experiments were performed on adult female Sprague Dawley rats, weighing between 250-300 g (Élevage JANVIER®, Centre d'Élevage Roger JANVIER, Le Genest Saint Isle, France), singly housed in smooth-bottomed plastic cages in a colony room maintained on a 12-h light/dark cycle and at 22 °C. Food (rat chow, Safe®, Augy, France) and water were available *ad libitum*. The weight of the rats was daily controlled. In order to accustom the animals to the laboratory environment, an acclimation period of 2 weeks was allowed before the initiation of the experiment.

2.2. Ethical approval

Nasal olfactory stem cells were obtained from a healthy donor informed about the study and the study design. He was also well informed about the advantages and disadvantages of participation. The biopsies were conducted in accordance with the Declaration of Helsinki and were approved by the local ethical committee (*Comité de Protection des Personnes*) of Marseille (IRB00005048). The donor provided its written informed consent to participate in this study.

Animal anesthesia and surgical procedures were performed according to the French law on animal care guidelines and were approved by animal Care Committees of *Aix-Marseille Université* (AMU) and *Centre National de la Recherche Scientifique* (CNRS). Individuals conducting the research were listed in the authorized personnel section of the animal research protocol or added to a previously approved protocol (License n°A13.013.06). Furthermore, experiments were performed following the recommendations provided in the Guide for Care and Use of Laboratory Animals (U.S. Department of Health and Human Services, National Institutes of Health) and in accordance with the European Community's council directive of 24 November 1986 (86/609/EEC), the ARRIVE Guidelines and the U.K Animal (Scientific Procedure) Act,. 1986. All these guidelines were carefully followed. No clinical sign of screech, prostration, hyperactivity, anorexia and no paw-eating behavior were observed through the study. If an animal had presented such a sign, it would have been sacrificed.

2.3. PNIPAAM-g-PEG synthesis and characterization

Copolymer synthesis. Poly(*N*-isopropylacrylamide)-co-poly(ethylene glycol)] methacrylate [p(NIPAAm-co-PEGMA)], also denoted as PNIPAAm-*g*-PEG, was synthesized by radical copolymerization of N-isopropylacrylamide (NIPAAm, Sigma Aldrich Merck, Saint Quentin Fallavier, France) with poly(ethylene glycol) methacrylate (PEGMA). PEGMA was first synthesized through reaction of polyethylene glycol monomethylether (Me-PEG-OH, Sigma Aldrich Merck) with methacryloyl chloride (Sigma Aldrich Merck). In brief, 10 g (5 mmol) of Me-PEG-OH (M_n = 2000 g mol^{-1}) was allowed to react with 5.2 g (49.7 mmol) of methacyloyl chloride (added dropwise) in 100 ml of dichloromethane (DCM), in presence of 7 ml (50.2 mmol) of triethylamine (TEA, Acros Organics, Illkirch, France). After 20 h under stirring at room temperature, DCM was removed under reduced pressure and the crude product was diluted with tetrahydrofuran (THF, VWR International S.A.S, Fontenay-sous-Bois, France). After filtration of the TEA salts, the crude solution was precipitated in 90% diethyl ether and 10% ethanol mixture, and dried under vacuum; ^{1}H NMR ($CDCl_3$): δ 1.95 (s, 3H, -C-CH_3), 3.38 (s, 3H, O-CH_3), 3.64 (s, 180H, -CH_2-), 4.29 (t, 2H, -CH_2-OC(O)-), 5.57 and 6.13 (s, 1H + 1H, -CH_2 = C).

For copolymerization, NIPAAm (3.68 g), PEGMA (0.263 g) and azobisisobutyronitrile (AIBN, Sigma Aldrich Merck) initiator (0.10 g) were dissolved in methanol (30 ml) in a two-neck round-bottom flask fitted with a septum and a reflux condenser, and the solution degassed for 30 min by argon bubbling. The flask was then immersed in an oil bath at 68 °C, and the polymerization allowed to run for 20 h. After reconcentration of the mixture by methanol evaporation under reduced pressure, the copolymer was precipitated twice in diethyl ether and dried under vacuum.

Copolymer characterization. Polymers were characterized by ^{1}H NMR in chloroform-d ($CDCl_3$) or in deuterated dimethyl sulfoxide (DMSO-d_6) with Bruker Advance 400 MHz spectrometer, and by size exclusion chromatography (SEC) using a Varian PL-GPC 120 apparatus, composed of a robotic autosampler (PL-AS-MT, Agilent Technologies, Les Ulis, France), a pump (Agilent 1100 series, Agilent Technologies), a degasser, an injection valve, a column oven and a refractive index (RI) detector. The following columns were used: one pre-column and two PL Resipore columns (300 mm Å ~ 7.8 mm). The injection loop, the columns and the RI detector were in the same oven thermostated at 70 °C. The eluent was a solution of 0.1 M LiBr in N,N-dimethylformamide (DMF) filtered through a 0.45 µm nylon membrane and the flow rate was fixed at 0.7 ml min^{-1}. The samples were prepared in a mixture of eluent and toluene (0.25 vol%) as the flowmarker, filtered through a 0.2 µm nylon filter (Interchim) and placed in an autosampler preheated at 50 °C. The sample concentration was 0.25 wt%. Calibration curve were established with poly(methyl methacrylate) (PMMA, Agilent Technologies). Lower critical solution temperature (LCST) of the copolymer was determined by dynamic light scattering analysis 0.6 wt% copolymer solution in PBS (pH 7.4). The hydrodynamic diameter and the count rate were measured using a Zetasizer Nano ZS apparatus (Malvern Panalytical SARL, Orsay, France). After equilibration at 25 °C, the temperature was incremented in steps of 1 °C until 40 °C. For each step, an equilibration period was fixed at 2 min.

Then, the copolymer was dissolved at 13.7 wt% in PBS and heated to 37 °C, at which the hydrogel quickly formed. Rheological properties of the hydrogel at 37 °C were analyzed with a rheometer (MCR 302, Anton Paar S.A.S., Les Ulis, France) equipped with a 25 mm diameter aluminum parallel disks. A volume of 0.6 ml of copolymer solution at 13.7 wt% in PBS was charged on the inferior disk at 20 °C. The solution was then heated to 37 °C to form a hydrogel with a gap width of 0.9 mm. The complex shear modulus ($G = G' + iG''$) was then measured as a function of frequency by dynamically shearing the hydrogel at a fixed strain of 1% over the frequency range 0.1–100 rad s^{-1} at 37 °C. All measurements were performed in a dry air atmosphere.

2.4. Survival and proliferation of nasal olfactory ecto-mesenchymal stem cells

Before evaluating the *in vivo* functional performance of the PNIPAAm-*g*-PEG hydrogel, the biocompatibility of the hydrogel was assessed *in vitro* on cell cultures. Nasal biopsies were immediately placed in growth medium containing DMEM/Ham F12 supplemented with 10% foetal bovine serum (FBS) and 100 units/ml of penicillin and 100 µg/ml of streptomycin (Invitrogen®, Thermo Fisher Scientific, Life Technologies SAS, Courtaboeuf, France). Olfactory ecto-mesenchymal stem cells were purified from the lamina propria and belong to the subfamily of ecto-mesenchymal stem cells as described before [80]. Briefly, the biopsies were incubated in a Petri dish filled with 1 ml of dispase II solution (2.4 IU/ml), for 1 h at 37 °C. Next, the olfactory epithelium was removed from the underlying lamina propria using a micro spatula. Once purified, the lamina propria was cut into small pieces with two 25 gauge needles and transferred into a 15 ml tube filled with 1 ml of collagenase IA. After a 10 min incubation at 37 °C, the tissue was mechanically dissociated and the enzymatic activity was stopped by adding 9 ml of Ca-free and Mg-free PBS. After centrifugation at 200*g* for 5 min, the cell pellet was resuspended in DMEM/Ham F12 culture medium, supplemented with penicillin/streptomycin and 10% fetal calf serum, and plated on plastic culture dishes. The culture medium was renewed every 2–3 days.

In order to quantify survival and proliferation of olfactory mesenchymal stem cells when loaded in the PNIPAAm-*g*-PEG, we

performed a gel spot assay. Hydrogel was diluted into sterile PBS in order to make a 13.7% solution. After passaging with trypsin, cultivated olfactory mesenchymal stem cells were collected, centrifuged and counted. In each well, 40,000 stem cells were loaded in 50 µl of the gel, at room temperature, and the plates were immediately transferred into a 37 °C incubator to allow each spot to solidify. The Petri dishes were then gently filled with serum-containing medium, renewed every 2/3 days. On Day 3, 6, 14 and 21, cells were collected and stained with Trypan blue before being quantified, using a Malassez counting chamber.

2.5. Protocol design and experimental groups

Thirty five animals were randomly assigned to the 3 following groups: 1) SHAM (n = 5), surgery was performed but without spinal cord injury, 2) Lesion group (n = 15), a C2 cervical hemisection was performed, 3) Lesion + PNIPAAM group (n = 15), a C2 cervical hemisection was followed by an immediate injection of PNIPAAm-*g*-PEG hydrogel in the lesion cavity.

Five animals of the Lesion and Lesion + PNIPAAM groups were sacrificed two weeks after the SCI to evaluate the endogenous inflammation at the lesion site. For other animals (n = 25), sensory and motor recovery in the anterior and posterior legs were followed during 3 months after the injury and injection of the hydrogel into the lesion cavity by using 4 behavioral tests. Then, at Month 3, spinal reflexivity and physiological adjustment to muscle fatigue were evaluated and the spinal cords were collected for assessing of the presence of the hydrogel within the lesion cavity and axonal growth.

2.6. Surgery

Animals were anesthetized with a 3% isoflurane (Isoflurin®, Axience Santé Animale SAS, Pantin, France) in oxygen (1 l min^{-1}) and placed in a stereotaxic frame. Under aseptic conditions, surgery was performed as previously described [81,82]. In the SHAM group, following a midline dorsal incision, the superficial muscles were retracted to expose the cervical vertebrae. Then, a laminectomy was performed without affecting the integrity of the spinal cord. In the two other groups, using microscissors the dura was incised and the left side of the C2 spinal cord was hemisected from the midline to the lateral part. This high cervical spinal cord hemisection interrupts descending tracts as well as propriospinal pathways to thoracic and lumbosacral segments [83,84]. It induces a central deafferentation of the phrenic motoneurones and a functional quiescence of the ipsilateral hemidiaphragm as well as dysfunction of muscles of ipsilateral forelimb and muscles of both hindlimbs [85].

Using a micropipette, 2 × 10 µl of sterile PNIPAAm-*g*-PEG were injected into the lesion cavity of animals from the Lesion + PNIPAAM group. After waiting a few minutes, gelation of the hydrogel *in situ* was observed. In all operated animals, muscles and skin were sutured (Vicryl® 3-0, Ethicon, Issy Les Moulineaux, France) in anatomical layers and the wound was disinfected with an antiseptic (Betadine®, 5%, Meda Pharma, Paris, France) and saline (2 ml of 0.9%) was injected subcutaneously. Furthermore, all animals were kept in a heated room overnight and treated during one week post-surgery with buprenorphin (0.03 mg/kg, Buprécare®, Axience Santé Animale SAS). Animal hydration and gastrointestinal function were monitored twice a day and bladders were manually expressed when necessary. Antibiotic (Amoxicillin trihydrate, 45 mg/ml, Synulox®, Zoetis SA, Malakoff, France) were preventively given for two weeks following surgery to prevent any infection.

2.7. Endogenous inflammation

Two weeks post-lesion, to evaluate the endogenous inflammation and the effect of hydrogel injection at the lesion site, animals from Lesion and Lesion + PNIPAAM groups were sacrificed with a lethal dose of anesthetic (Pentobarbital sodium, 390 mg/kg, i.p., Euthasol® Vet., Dechra Veterinary Products S.A.S., Montigny-le-Bretonneux, France). A segment of spinal cord extending 5 mm rostral and caudal to the injury site was quickly removed and frozen immediately in isopentane and stored at -80 °C until further processing. The spinal cord tissues were homogenized separately in 1 ml of Phosphate Buffer Sodium (PBS) for 30 s by a handheld homogenizer (Ika Ultra Turrax® disperser, Fisher Scientific SAS, Illkirch, France), which has connecting plastic pestle tips that homogenize the tissue through vibrating motions. Then, the resulting mixtures were centrifuged (centrifuge Sigma 2-16 PK Centrifuge Fisher Scientific SAS, Illkirch, France) for 12 min (2000 × *g*, 4 °C) and a fraction (50 µl) of the supernatant of the homogenate containing soluble proteins was used to evaluate inflammation. The concentrations of IL-1β, IL-6 and TNF-α, in spinal cord tissue homogenates were measured using enzyme-linked immunosorbent assay (ELISA) kits containing specific antibodies (RAB0272, RAB0311 and RAB0480, Sigma Aldrich®, Saint-Quentin Fallavier, France), according to the manufacturers' instructions. Each sample was analyzed twice. Absorbance was determined using a microplate reader (Multiskan® Microplate Photometer, Thermo Fisher Scientific, Life Technologies SAS, Courtaboeuf, France) at a wavelength of 450 nm. The concentration of inflammatory mediators in each sample was obtained by comparison with samples containing known amounts of inflammatory mediators. Then, a curve linking the concentration to the measured absorbance was computed. Concentrations were based on the amount of tissue weighed before homogenization and expressed in pg per g of spinal cord.

2.8. Behavioral tests

Before surgery, in order to decrease inter-individual differences, all animals were familiarized with the 4 behavioral tests, 3 days per week during two weeks. This acclimation period allows animals to reach optimal performances. The day before surgery, reference values (PRE-) of each test were recorded. Then, during 12 weeks (W1 to W12), the tests were performed, once a week, by the same experimenter in order to obtain more reproducible and reliable data.

BBB-derived test (Martinez's Scale). Deficits and recovery of sensorimotor functions were assessed using a tool derived from the BBB test [86]. Briefly, animals were place in an open-field environment made of a circular Plexiglas® enclosure arena (95-cm diameter, 40-cm wall height) with an anti-skid floor. The scale comprises eight categories that allow for separate evaluation of the forelimbs and hindlimbs: articular movements of the affected limbs, weight support, digit position, paw placement, orientation and movement during stepping, limbs coordination and tail position. A total maximum score of 20 points indicates normal locomotion or full functional recovery. In order to assess separately forelimb and hindlimb functions, animal movements were video-recorded during sessions of 4 min duration (MV 830i; Canon®, Courbevoie, France) and analysis was carried out later on.

Ladder climbing test. From 1 week after surgery, cortical control of fine sensorimotor coordination was tested during a climbing task. Climbing a ladder is an easily acquired spontaneous response, requiring neither compulsion nor reward. As previously described [82,87,88], this test was used to evaluate the sensorimotor capacities to correctly grip the rung while rats climbed up an inclined ladder (10 cm × 150 cm; rod diameter: 0.4 cm; distance inter-rods: 2 cm) at a 45° angle. The climbing test was repeated one time a week for twelve successive weeks. Unoperated animals climb readily, with all four paws locating and grasping the rods without fault. In all operated animals, the forepaw on the operated side showed varying degrees of difficulty in locating the ladder rods. As a result, a climbing score ranging from 0 (without success, i.e., 0 grip with the forepaw ipsilateral to the lesion) to 40 (animal climbed 40 rods of the ladder without faults, i.e., 20 grips with the forepaw ipsilateral to the lesion) was calculated and

normalized to the maximal score. The mean ratio obtained at each session was expressed as percentage of the mean ratio obtained at week 0 (PRE-). All the details regarding how to calculate the score are given in a previous article [82].

Grip strength test. As previously described the force exerted by both forepaws/forelimbs was measured using a grip force tester [Grip Strength Tester (GST) bio-GT3, Bioseb apparatus, Vitrolles, France] [82,89]. Animals were tested once a week by the same experimenter in order to obtain more reproducible and reliable data. Four maximal forces (in grams) were averaged over 3-5 trials. Results were normalized by the weight (in grams) of the animal (force/weight ratio) and expressed as percentage of the ratio obtained at week 0 (PRE-).

Tape removal test. In order to test the sensory function, rats were placed individually in a transparent rectangular cage (30 cm × 20 cm) and a piece of adhesive tape (Scotch®, 3 M, Pontoise, France) of 25 mm^2 (5 × 5 mm) was affixed to the palm of the forelimb [90,91]. This adhesive tape causes discomfort for the animal that will remove it quickly with his mouth. This behavior implies correct paw and mouth sensitivity (time-to-contact) and correct dexterity (time-to-remove). The time from the tape was affixed until it was detected by the animal was measured in three individual trials to calculate the mean sensing time. The left (ipsilateral to the lesion) and right forelimbs were separately tested and the asymmetric score was calculated using the following formula: $T_L/(T_L + T_R)$, where T_L and T_R were the mean sensing time measured in the left and in the right forelimb, respectively. The asymmetric score ranges from 0 (full sensory deficit on the right forelimb compared to the left forelimb) to 1 (full sensory deficit on the left forelimb compared to the right forelimb). A score of 0.5 indicates symmetry of tactile sensitivity between the two forelimbs. If an animal did not detect the tape, the trial was stopped after 180 s and this value was taken as the time recorded.

2.9. Electrophysiological recordings

Twelve weeks post-injury, animals were anesthetized by intramuscular injection of ketamine (62.5 mg/kg^{-1}, 100 mg m^{-1}, Ketamine 1000®, Virbac®, Carros, France) and xylazine (3.125 mg kg^{-1}, 20 mg ml^{-1}, Xilasyn®2, Virbac®), and prepared for electrophysiological recordings as previously described [81,82]. Briefly, the *ulnar* nerve from the left forelimb was dissected free from surrounding tissues for stimulation. Then, *Flexor Digitorum* muscle from the left forelimb and *Tibialis anterior* muscle from the left hindlimb were exposed for electromyographic (EMG) recording and stimulation, respectively.

M- and H-waves. As previously described [25,81,82,92–98], the H-reflex rate sensitivity (i.e., the decrease in reflex magnitude relative to repetition rate) was analyzed. In order to calculate the H-reflex rate depression, the H_{max}/M_{max} ratio obtained at the stimulation frequency of 1, 5 and 10 Hz was expressed as a percent of the H_{max}/M_{max} ratio obtained at the baseline frequency of 0.3 Hz.

Physiological reflexes. Ventilatory adjustments were measured after activation of metabosensitive afferent fibers by *Tibialis anterior* muscle repetitive stimulation and under regional circulatory occlusion [25,81,82,92,99]. Thus, changes in ventilatory frequency after electrically-induced muscle fatigue (EIF) was expressed in percent [Δcycle/min (%)] of the mean cycles recorded 2 min before muscle stimulation.

2.10. Euthanasia and histological analysis

According to ethical recommendations, at the end of each series of electrophysiological recordings, the animal was sacrificed with an overdose of anesthetic (Pentobarbital sodium, 390 mg/kg, i.p., Euthasol® Vet.) and the C1-C5 spinal segment was removed, rinsed in cold phosphate buffer saline (PBS) 0.1 M and frozen on dry ice. All samples were then stored at -80 °C. Then, 50-μm thick horizontal sections were performed using a cryostat (CM1950, Leica Biosystemes S.A., Nanterre, France). Slices were collected on SuperFrost Ultra Plus™ (Thermo Fisher Scientific) glass slide and sampled every five sections. After a 15 min dip in a solution containing 4% of paraformaldehyde followed by 4 rinsing in cold PBS, the spinal sections were used to perform double indirect immunofluorescence detection against Glial Fibrillary Acidic Protein (GFAP, Agilent Technologies, Inc., Les Ulis, France) and 70 kDa Neuro-Filament (NF, Agilent Technologies, Inc.). Before incubation of antibodies, sections were subjected to several pretreatments to improve antibody-binding specificity and to reduce nonspecific signals. They were incubated in 0.1 M lysine (Sigma Aldrich Merck) and then permeabilized with 0.3% TritonX100 (Sigma Aldrich Merck). Nonspecific sites were blocked with 2% bovine serum albumin (Sigma Aldrich Merck). Incubations were carried out for 48 h at 4 °C with the primary antibodies diluted in PBS including 2% bovine serum albumin and 0.3% TritonX100 at the following dilutions: rabbit antibody against GFAP (1/500, Agilent Technologies, Inc.) and mouse antibody against NF (1/1000, Agilent Technologies, Inc.). After rinses with PBS, sections were incubated for 2 h at room temperature with a goat anti-rabbit Ig G and a goat anti-mouse Ig G secondary antibodies (1/200) conjugated a red- and green-fluorescent dyes (Alexa Fluor® 594 and 488, Invitrogen®, Molecular Probes® Product Brands), respectively. Sections were observed by epifluorescence optical microscopy using an Eclipse E600 microscope (Nikon®, Champigny-sur-Marne, France). Measurements and microphotographs were performed with an analyzing software (Lucia®, Lim Laboratory Imaging s.r.o., Praha, Czech Republic).

2.11. Statistical analysis

Analysis of ELISA data was performed with a t-test. Results obtained from behavioral tests and electrophysiological recordings were compared between all experimental groups. Data processing was performed using a software program (SigmaStat®, San Jose, CA, USA). Normal data distribution was verified and a two-way ANOVA (group factor x time factor or stimulation frequency factor) for repeated measures was used to compare groups with each other and over time for behavioral scores and over stimulation frequency for H_{max}/M_{max}. Then, statistics were completed with a multiple-comparison *post-hoc* test (Student-Newman-Keuls method). Wilcoxon and Mann-Whitney tests were used to determine the ventilatory increase after the stimulus was applied and for histological analysis, respectively. Data were expressed as mean ± SEM. Results were considered significant if the p-value fell below 0.05.

3. Results

3.1. PNIPAAM-g-PEG synthesis

The copolymer composition (94/6 wt% in NIPAAm/PEG, determined from ^{1}H NMR integration, Fig. 1A) and molecular weight (83000 g mol^{-1}, Đ = 1.9, from SEC) were adjusted to ensure both suitable LCST (33 °C, sufficiently below 37 °C, Fig. 1B) and chain entanglement. At 13.7 wt% in physiological solution (PBS, pH 7.4), hydrogel formation occurred instantaneously at 37 °C (Fig. 1C). The storage modulus (G′) and loss modulus (G″) of the copolymer hydrogel were investigated at 37 °C by varying angular frequency from 0.1 to 100 rad s^{-1} to assess the rheological behavior of the hydrogel in conditions close to *in vivo*. Values were in the range 25–50 kPa and 17-20 kPa, respectively (Fig. 1D).

3.2. Animals

All operated rats survived until the electrophysiological phase or during the two weeks (rats used to evaluate endogenous inflammation) following the surgery. Except the 10 rats sacrificed 2 weeks after the SCI, all animals underwent all weekly behavioral tests. Their weight did not drop throughout the experiment. The injury resulted in pronounced

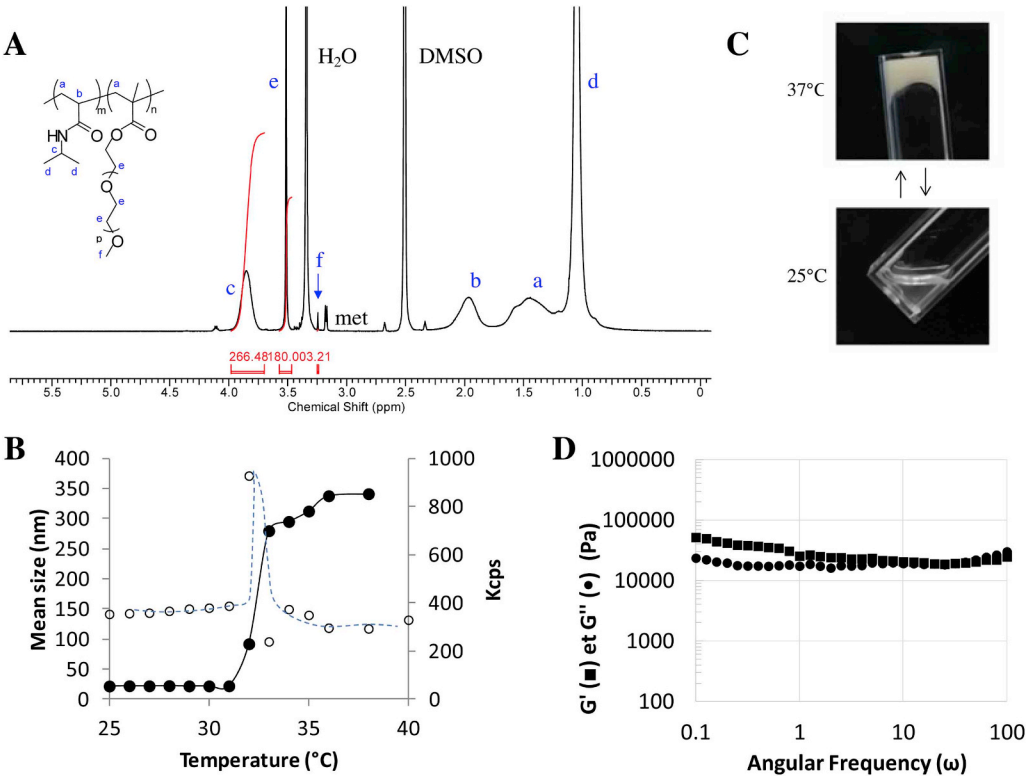

Fig. 1. *Hydrogel preparation and characterization.* **A.** 1H NMR of the PNIPAAm-*g*-PEG copolymer in DMSO-d_6 (met. = methanol traces; -C-CH_3 and -CH_2-OC(O)- protons from the original PEGMA are overlapped); **B.** LCST of the copolymer determined by DLS (PBS, pH 7.4); **C.** Hydrogel formation at 37 °C (13.7 wt% in PBS, pH 7.4); **D.** Storage modulus (G′) and loss modulus (G″) of the copolymer hydrogel (13.7 wt% in PBS, pH 7.4) at 37 °C.

motor deficits in the ipsilateral limbs and in bilateral sensory deficits. Furthermore, the ipsilateral hemidiaphragm became functionally quiescent. The high cervical spinal cord hemisection interrupted motor descending pathways as well as propriospinal pathways to thoracic and lumbosacral segments. It also interrupted sensory ascending pathways.

3.3. Survival and proliferation of olfactory ecto-mesenchymal stem cells

Measurement of the number of cells from the day (D0) of seeding to the fourteenth day (D14) revealed that from the sixth (D6) day the number of cells was significantly higher (D6, $p < 0.01$; D14, $p < 0.001$; D21, $p < 0.001$) than that at D0. Within the 21 days on culture the number of cell increased exponentially and cells were 5 times more numerous at D21 (267800 ± 12635 cells) when compared to D0 (40000 cells) (Fig. 2).

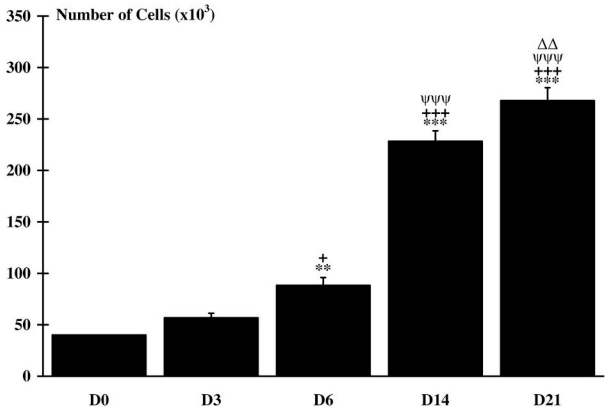

Fig. 2. *Cell survival and proliferation.* Measurement of the number of cells, from the day of seeding (D0) to D21, reveals an exponential increase. Significant differences at D0, D3, D6 and D14 are indicated by *, +, ψ and Δ, respectively. (1 symbol, $p < 0.05$; 2 symbols, $p < 0.01$ and 3 symbols, $p < 0.001$).

3.4. Endogenous inflammation

Measurement of IL-1β, IL-6 and TNF-α levels at the lesion site did not reveal difference between Lesion and Lesion + PNIPAAM groups indicating that the hydrogel did not produce additional inflammation within the 2 weeks following injection (Fig. 3).

3.5. Behavioral tests

No difference was observed from PRE-measurements until week-12 (W12) in the SHAM group for the 4 behavioral tests.

BBB-derived test (Martinez's Scale). Analysis of the BBB scores during the 12 weeks following the surgery revealed that the SHAM group had relatively stables values closed to the maximal PRE-values. However, in the two lesioned groups, the scores dropped significantly ($p < 0.001$) at Week 1 (W1) post-surgery and, although remaining lower ($p < 0.001$) than the SHAM group, recovered from the 2nd to the 12th week with higher ($p < 0.001$) scores for Lesion + PNIPAAM group than Lesion group (Fig. 4).

Ladder climbing test. Analysis of the climbing scores during the 12 weeks following the surgery revealed that the SHAM group had relatively stables values closed to the maximal PRE-values. However, in the two lesioned groups, the scores dropped significantly ($p < 0.001$) at W1 post-surgery. Throughout the 3 months post-surgery, the scores in the two lesioned groups were lower than in the SHAM group. Furthermore, in the Lesion + PNIPAAM group a recovery was observed from the 3rd to the 12th week with higher (W3, $p < 0.05$; W4 to W12, $p < 0.001$) scores for the Lesion + PNIPAAM group compared to the Lesion group. Scores of the Lesion group remained relatively stable from WI to W12 (Fig. 5).

Grip strength test. Analysis of the force developed in each forelimb indicated that the force dropped significantly ($p < 0.001$) at W1 after the spinal lesion in the ipsilateral side (left limb) in the Lesion and Lesion + PNIPAAM groups compared to the force developed by the forelimbs of the SHAM group or controlateral forelimb of the respective group. Furthermore, in the lesioned groups, the force of the ipsilateral

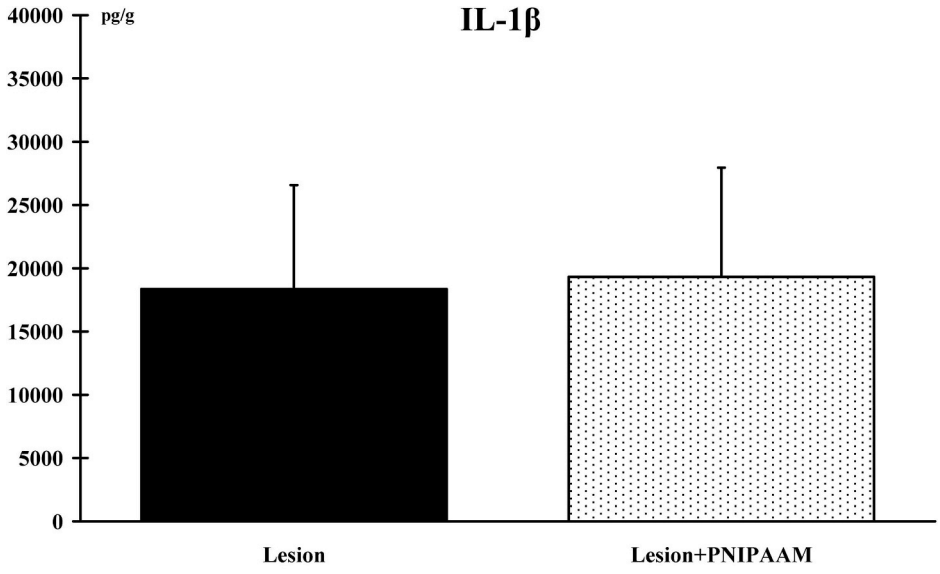

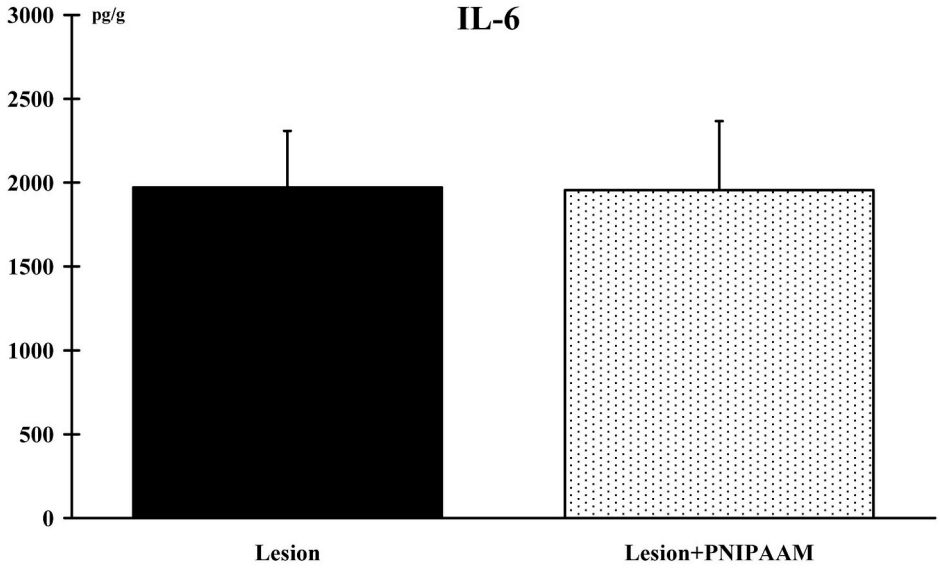

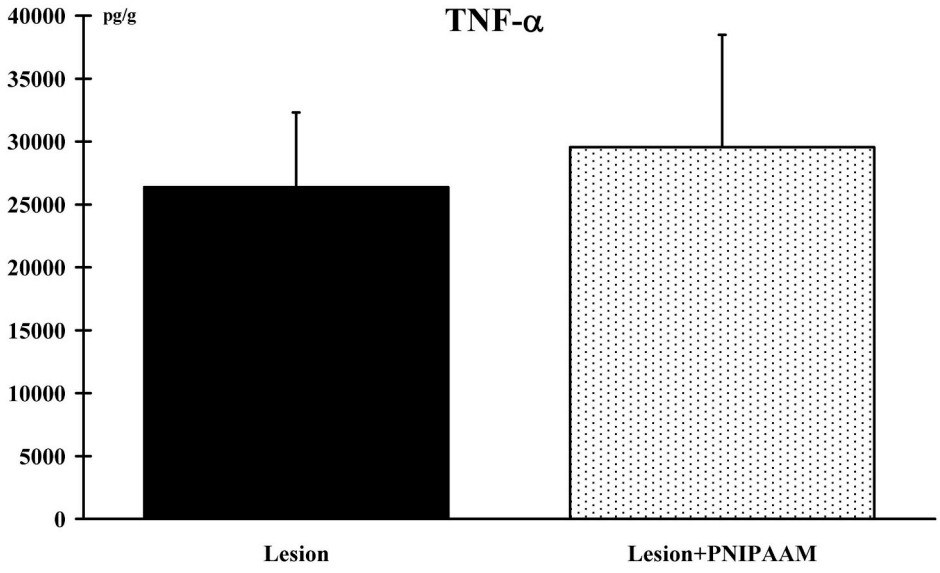

(caption on next page)

Fig. 3. *Inflammatory reaction at the lesion site*. Comparison of IL-1β, IL-6 and TNF-α levels at the site of injury in the Lesion and Lesion + PNIPAAM groups, two week post-injury, does not reveal any additional inflammation when the hydrogel is added.

forelimb to the lesion remained lower during the 12 weeks of experiment. However, in the Lesion + PNIPAAM group, a recovery was observed from the 5th to the 12th week (W5 and W6, $p < 0.01$; W7 to W12, $p < 0.001$); the force developed in the left forelimb was significantly higher than that developed in the left forelimb of the Lesion group (Fig. 6).

Tape removal test. Analysis of the asymmetric score indicated that the mean sensing time measured in the left forelimb (ipsilateral to the lesion) increased drastically after the C2 hemisection. However, while asymmetric scores were measured in the Lesion and Lesion + PNIPAAM groups until the end (W12) of the experiment, from the W3 to the W12, the score became significantly lower in the Lesion + PNIPAAM group than in the SHAM group (Fig. 7).

3.6. Electrophysiological recordings

M- and H-waves. In the left (ipsilateral) foreleg, the value of the H_{max}/M_{max} ratios measured at the baseline stimulation (0.3 Hz) were 0.38 ± 0.06, 0.46 ± 0.11 and 0.37 ± 0.06 for SHAM, Lesion and Lesion + PNIPAAM groups, respectively. The ratio of the Lesion group was significantly higher ($p < 0.01$) than ratios of other groups. Furthermore, frequency-dependent values of H-reflex analysis (Fig. 8) indicated that when the frequency of stimulation was increased to 1 Hz, the H_{max}/M_{max} ratio slightly decreased for the SHAM (91.42 ± 3.15%) and Lesion + PNIPAAM (94.49 ± 3.02%) groups and increased for the Lesion group (105.04 ± 2.87%). These changes were not significantly different than the ratio measured at 0.3 Hz. Moreover, no statistical difference was found between groups. At 5 Hz stimulation, a significant ($p < 0.001$) decrease was observed in the SHAM group (78.35 ± 3.56%) compared to the values obtained at 0.3 Hz and no significant change was noted in the two other groups (Lesion: 108.29 ± 6.81% and Lesion + PNIPAAM: 89.87 ± 4.90%). However, comparison between groups indicated a significant difference between the Lesion group and the other two groups (SHAM: $p < 0.001$ and Lesion + PNIPAAM: $p < 0.01$). At 10 Hz stimulation, ratios of SHAM (61.04 ± 6.89%) and Lesion + PNIPAAM (76.90 ± 7.38%) groups decreased significantly ($p < 0.001$) compared to the values obtained at 0.3 Hz. Comparisons between groups showed significant difference between the lesion group and the two other groups (SHAM: $p < 0.001$ and Lesion + PNIPAAM: $p < 0.05$). Finally, a significant difference ($p < 0.05$) was also noted between the SHAM and the Lesion + PNIPAAM groups. These last two groups had the same response profile, namely a decrease of the H_{max}/M_{max} ratio with the increase of the stimulation frequency and from 1 Hz. This result can be correlated with functional outcome in animals receiving the hydrogel.

Physiological reflexes. Ventilatory frequency measured after left (ipsilateral) peroneal nerve stimulation was only significantly ($p < 0.01$) increased in the SHAM group (+6.23 ± 1.12%). Compared to the resting data, in the Lesion group a slight decrease (-5.20 ± 1.64%) was observed. In the Lesion + PNIPAAM group the slight increase (+0.5 ± 0.7%) was not significant. Comparison between groups indicated a significant difference ($p < 0.01$) between the SHAM group and the two other groups.

3.7. Histological analysis

Spinal damages are known to lead to the development of cavities surrounded by a glial scar called cysts. In animal receiving the hydrogel, histological analysis showed that all these cysts were filled up by the polymer. Beyond the stability of this substance, it was noted that no cell invaded the hydrogel. Glial processes only weakly colonized the hydrogel (Figue 9A). Some rare GFAP-immunoreactive (GFAP-Ir) processes have been observed on the periphery without ever entering more than 15 µm within the hydrogel. Regarding the neuronal processes, the NF-immunoreactive (NF-Ir) was still observable in the spare funiculi (Fig. 9B) but the density of NF-Ir fibers was strongly decreased in the glial scar (Fig. 9C). Only a few of these processes are detectable in this region. Conversely, numerous NF-Ir processes were visible within the hydrogel. These fibers were highly labeled and mainly exhibited a rostro-caudal orientation, as in the spare tissues.

4. Discussion

The aim of our research was to evaluate the therapeutic potential of

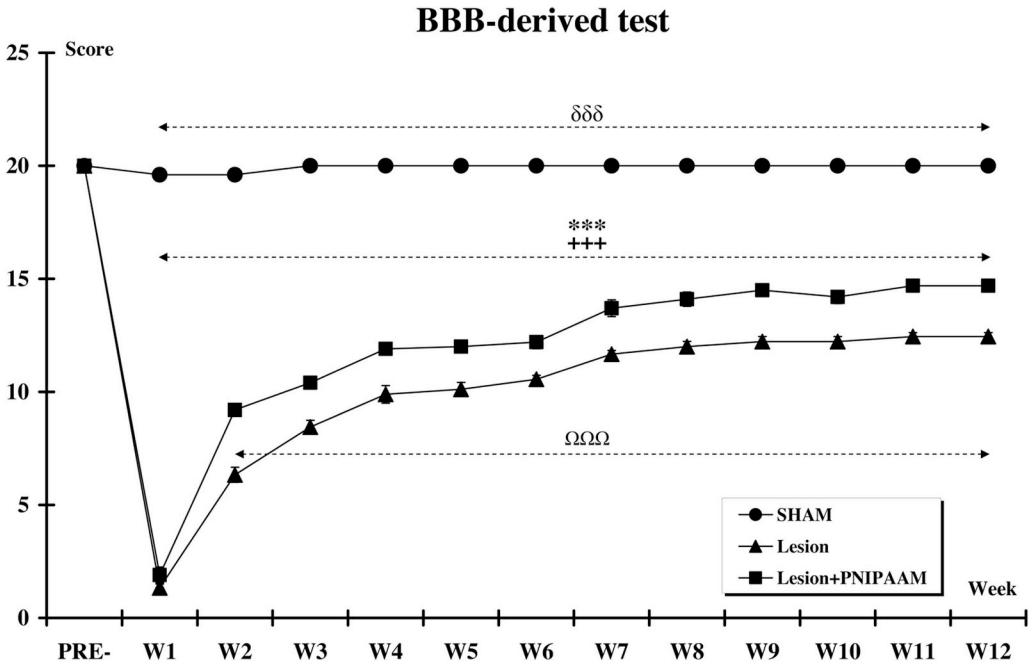

Fig. 4. *BBB-derived locomotor rating scale.* Significant difference in the BBB-derived scores is indicated by a * (Lesion group, PRE-*vs.* post-surgery), + (Lesion + PNIPAAM group, PRE-*vs.* post-surgery), δ (SHAM group *vs.* Lesion and Lesion + PNIPAAM groups) and Ω (Lesion group *vs.* Lesion + PNIPAAM group). (3 symbols, $p < 0.001$).

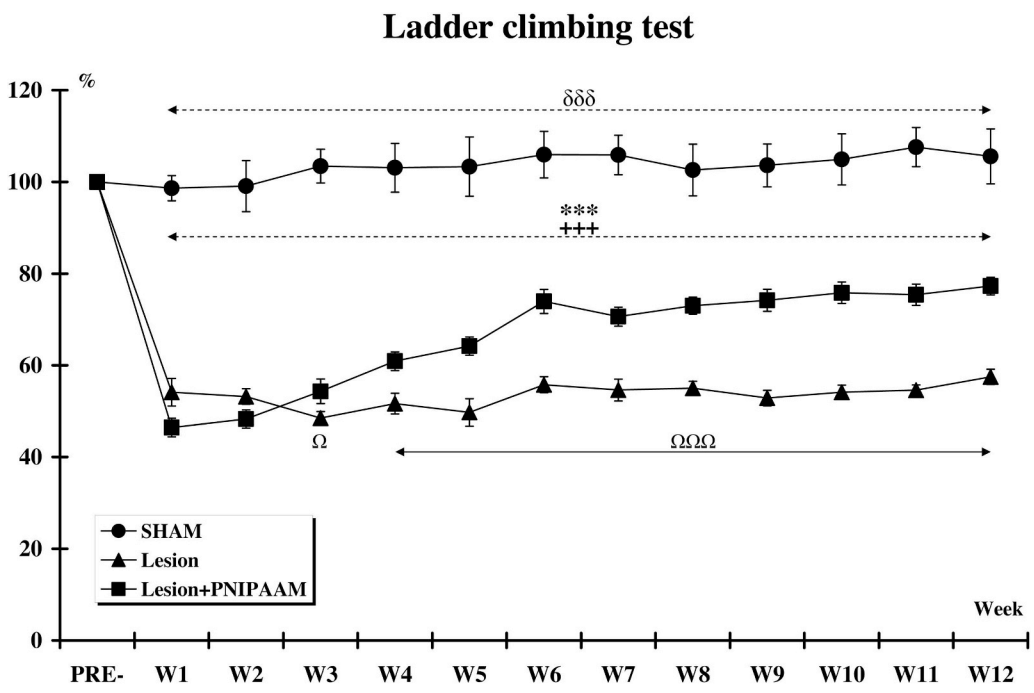

Fig. 5. *Ladder climbing test.* Significant difference in the climbing scores is indicated by a * (Lesion group, PRE-*vs.* post-surgery), + (Lesion + PNIPAAM group, PRE-*vs.* post-surgery), δ (SHAM group *vs.* Lesion and Lesion + PNIPAAM groups) and Ω (Lesion group *vs.* Lesion + PNIPAAM group). (1 symbol, $p < 0.05$ and 3 symbols, $p < 0.001$).

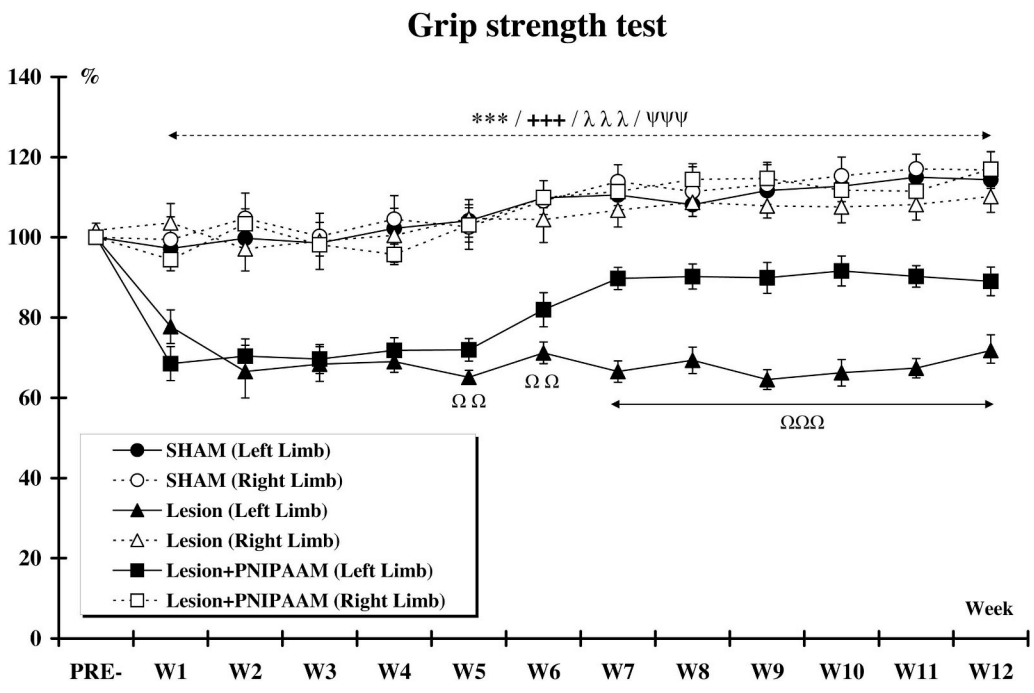

Fig. 6. *Grip strength test.* Significant difference in the maximal force developed in the forelimbs is indicated by a * (Lesion group, left forelimb, PRE-*vs.* post-surgery), + (Lesion + PNIPAAM group, left forelimb, PRE-*vs.* post-surgery), λ (Lesion group, left forelimb *vs.* SHAM group, left and right forelimbs and Lesion and Lesion + PNIPAAM groups, right forelimb), ψ (Lesion + PNIPAAM group, left forelimb *vs.* SHAM group, left and right forelimbs and Lesion and Lesion + PNIPAAM groups, right forelimb) and Ω (Lesion group, left forlimb *vs.* Lesion + PNIPAAM group, left forelimb). (2 symbols, $p < 0.01$ and 3 symbols, $p < 0.001$).

the poly(N-isopropylacrylamide)-poly(ethylene glycol) copolymer (PNIPAAm-g-PEG) after injection in a rat hemisectioned spinal cord. We hypothesized that a compatible synthetic hydrogel that fills the lesion cavity could limit the development of glial scar, allow axonal regeneration and accelerate post-traumatic functional recovery. For the first time, the current study demonstrates that human cells survive and proliferate when cultivated within the hydrogel. *In vivo*, measurement of cytokines (IL-1, IL-6 and TNF-α) indicates that hydrogel did not induce additional inflammatory reaction within the first 2 weeks post-injection in the lesion cavity. Motor and sensory recovery is enhanced in hydrogel-implanted animals and, at twelve weeks post-injury, analysis of the H-reflex reveals the restoration of the post-activation depression in grafted rats. Finally, neurofilament-positive axons invade the gel while astrocytes remain at the periphery.

4.1. PNIPAAm-g-PEG display mechanical properties suitable for spinal cord repair

Due to its suitable LSCT between room and physiological temperature (~32 °C), PNIPAAm is attractive for designing injectable hydrogels. However, its pronounced hydrophobicity above LCST requires introduction of hydrophilic moieties to ensure water retention and prevent gel shrinkage [100]. Our approach relied on a PNIPAAm copolymer grafted with PEG segments, yielding physical hydrogel upon PNIPAAm collapsing above transition temperature. We opted for physically cross-linked hydrogels instead of chemically based ones (e.g. using PEG diacrylates) [79] for enabling copolymer to be potentially excreted through renal clearance, even if the molecular weight of our copolymer (about 80 kg mol^{-1}) was slightly higher than commonly

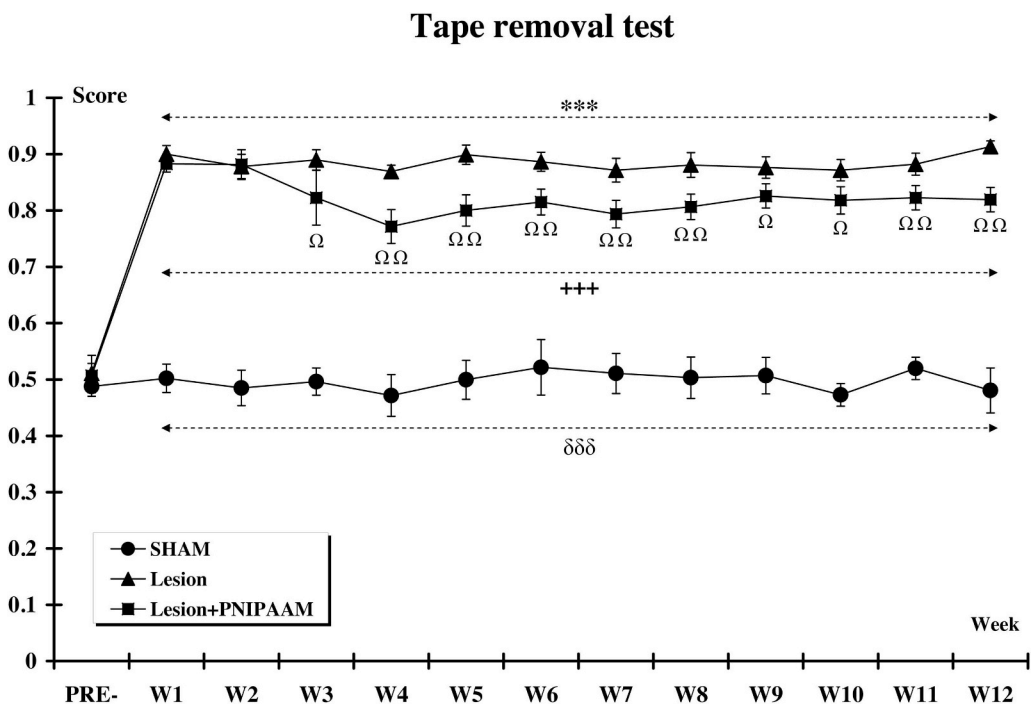

Fig. 7. *Tape removal test.* Significant difference in the asymmetric scores is indicated by a * (Lesion group, PRE-*vs.* post-surgery), + (Lesion + PNIPAAM group, PRE-*vs.* post-surgery), δ (SHAM group *vs.* Lesion and Lesion + PNIPAAM groups) and Ω (Lesion group *vs.* Lesion + PNIPAAM group). (1 symbol, $p < 0.05$; 2 symbols, $p < 0.01$ and 3 symbols, $p < 0.001$).

reported renal cutoff (≈70 kDA) to ensure sufficient mechanical properties [101]. The copolymer was obtained by radical copolymerization of NIPAAm and PEGMA and values of the storage modulus (G′) and loss modulus (G″) typically matched with those of spinal cord [102]. Thus, because of its mechanical properties, our hydrogel was a very good candidate to replace the spinal cord tissue lost during the mechanical injury.

4.2. PNIPAAm-g-PEG supports survival and proliferation of human stem cells in vitro

If NIPAAm monomer was considered as a toxic agent for living cells, there are conflicting opinions concerning the toxicity of the polymerized form of NIPAAM [103,104], known to be associated to concentration, temperature and incubation. However, in order to counteract its potential toxicity, PNIPAAm was combined with PEG. Thus, it was shown that PNIPAAm-*g*-PEG may support the survival of SH-SY5Y human neuroblastoma cells [105].

In this context, the first step in this process was to check the toxicity of the PNIPAAm-*g*-PEG hydrogel by seeding human olfactory ecto-mesenchymal stem cells (hOE-MSCs) in the hydrogel. Our results indicate that, within 21 days, the cells proliferated, reaching a five fold increase. This result confirms previous studies showing the potential of PNIPAAm-*g*-PEG 3-dimensional hydrogel to support the survival and development of human stem cells. Indeed, Comolli et al. [76] showed that PNIPAAm-*g*-PEG scaffolds are capable of supporting human bone

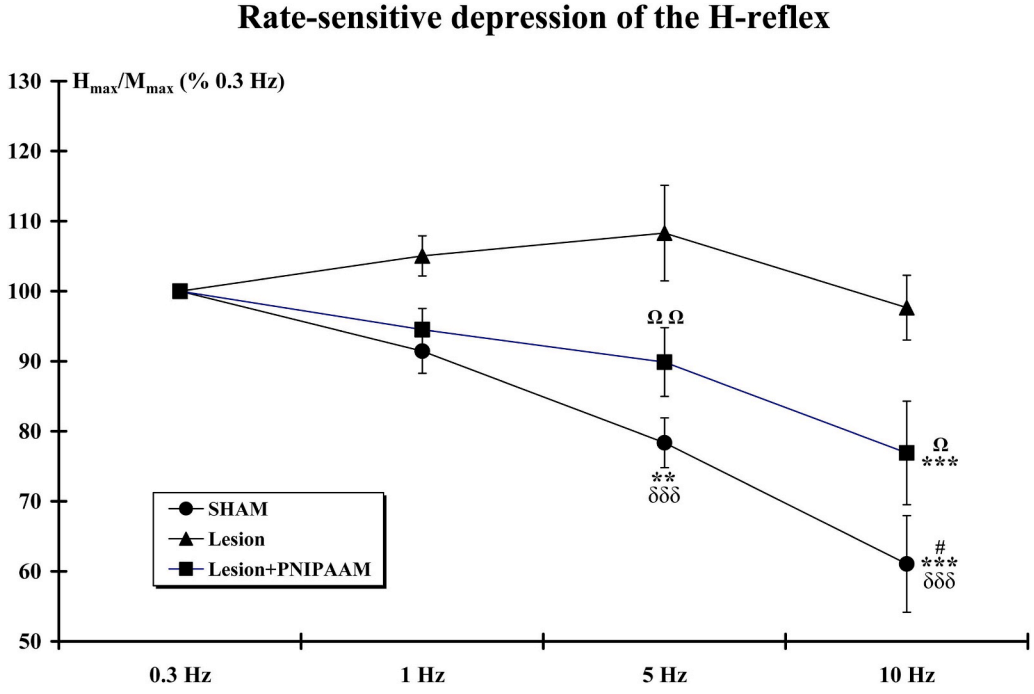

Fig. 8. *H-reflex recordings.* H-reflex rate sensitivity, measured after increasing the frequency of stimulation, shows similar profiles in the SHAM and the Lesion + PNIPAAM groups. Significant difference between the H_{max}/M_{max} ratio is indicated by a *. For a given frequency, significant difference between the SHAM and the lesion groups is indicated by a δ. Significant difference between the Lesion + PNIPAAM and the Lesion groups is indicated by a Ω. Significant difference between the SHAM and the Lesion + PNIPAAM groups is indicated by a #. (1 symbol, $p < 0.05$; 2 symbols, $p < 0.01$ and 3 symbols, $p < 0.001$).

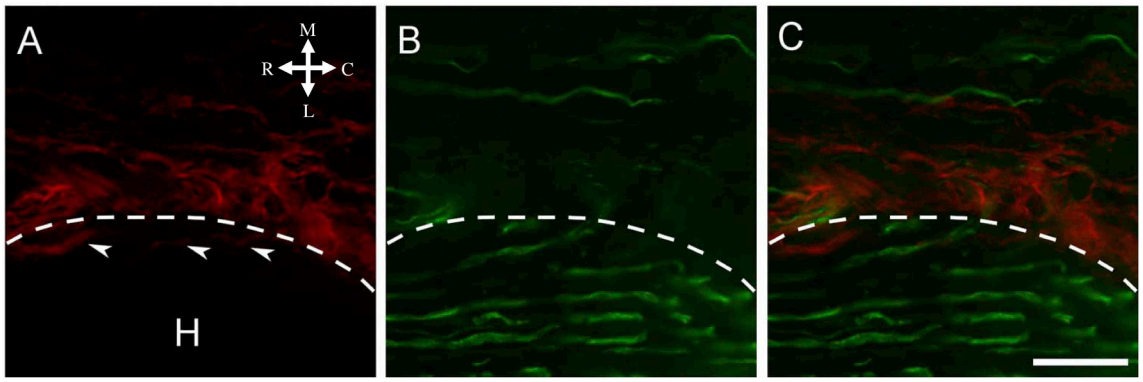

Fig. 9. *Histological assessment of neurite outgrowth in the hydrogel after SCI.* In the damaged spinal tissues, the cysts (delineated by the white dot line) were surrounded by the glial scar highlighted by an enhanced GFAP-Ir (red). The hydrogel (H) filled up all the cavities in the lesion site. While only a few glial processes (white arrows) colonized the hydrogel, up to 15 μm inside (A), NF-immunoreactive neurites (green) invaded the loaded gel (B). Interestingly, the rostro-caudal orientation of the fibers in the spared tissue was also observed in the hydrogel. By contrast, the NF-Ir in the glial scar was restricted to rare thin neurites (C). R: Rostral, C: Caudal, M: Medial, L: Lateral. Scale Bar: 50 μm. (For interpretation of the references to colour in this figure legend, the reader is referred to the Web version of this article.)

marrow stromal cell attachment and viability *in vitro*. More recently, it has been shown that striatal progenitors from human pluripotent stem cells (hPSCs) developed a medium spiny neurons-like phenotype when transplanted into a transgenic mouse model of Huntington disease [106,107]. The same group previous reported that midbrain dopaminergic neurons may differentiate from hPSCs when cultured in PNIPAAM-*g*-PEG hydrogel and transplanted into rat striatum [108,109].

4.3. PNIPAAm-g-PEG does not increase endogenous inflammation

The second step of our demonstration was to verify that our PNIPAAm-*g*-PEG hydrogel did not trigger an additional inflammation [110–113]. Implantation of the hydrogel had no negative influence on inflammation, suggesting that it could be a good candidate for spinal cord repair. Previous reports on that topic are conflicting. One study demonstrated that PNIPAAm-*g*-PEG hydrogel elicited a considerable inflammatory response when injected in the striatum [105]. Conversely, evaluating reactive macrophages and microglia levels (IBA-1 labeling), Conova et al. [78] reported that PNIPAAm-*g*-PEG hydrogel did not elicit a greater host inflammatory response than the commercially available Gelfoam® or Vitrogen PureCol® matrix known to be a biocompatible scaffold material.

Tunesi et al. [105] used ratios of PNIPAAm/PEG of 100/1.2 mg/ml, 200/1.2 mg/ml and 300/1.2 mg/ml (with NIPAAm: 10000 g/mol and PEG: 3350 g/mol), the hydrogel being here made of separated PNIPAAm and PEG homopolymer, namely PEG contents ranging from 0.4 to 1.2 wt% while Conova et al. [78], used a molar ratio of NIPAAm/PEG of 1000/1 (with PEG: 8000 g/mol) which corresponds to PEG content of 6.6 wt%, close to that of our hydrogel (6 wt%). Thus, it cannot be excluded that PEG in the hydrogel is beneficial to decrease the inflammation. Furthermore, in contrast to the hydrogel of Conova et al. (chemically cross-linked) [78], our hydrogel was physically cross-linked, which may further contributed to a reduced inflammation.

4.4. PNIPAAm-g-PEG improves sensory and motor recovery

As soon as the first week post-injury, the decline in sensori-motor score of the hemisected rats (Lesion and Lesion + PNIPAAM groups) was in accordance with previous studies showing the important deficit after identical spinal cord lesion [26,82,114]. Although some spontaneous improvements were noticed with BBB score, all behavioral (BBB-derived test, ladder climbing test, grip strength test, tape removal test) tests used in our study showed greater recovery in animal groups with an hydrogel immediately implanted after the spinal cervical (C2) cord hemisection. All scores were improved from W2/W3, except for the grip strength task mainly involving the motor pathways that showed improvement from W5. These results indicate that the matrix was beneficial when injected immediately after the spinal lesion suggesting that the hydrogel may 1) limit the extension of the lesion (secondary injury) and/or 2) restrain the formation of the glial scar preventing the axon regeneration and/or 3) promote the axon regrowth or sprouting from injury or spare axons. However, if comparison can be made between studies, results of our study (C2 hemisection, BBB-derived test) are not in accordance with results of a recent study showing no difference in BBB scores (BBB test) between animals with a moderated contusion injury at T9/T10 and animals with the same lesion receiving one-week post SCI a PNIPAAm-*g*-PEG hydrogel (PEG: 8000 g/mol, molar ratio NIPAAm/PEG: 1000/1) loaded with BDNF/NT3 [115]. In this model of thoracic lesion, the authors did not evaluate the efficacy of the hydrogel alone. Previously, it was shown that the same PNIPAAm-*g*-PEG hydrogel loaded with BDNF induced greater motor (single-pellet reach-to-grasp task, staircase-reaching task and cylinder task) recovery than PNIPAAm-*g*-PEG alone in a model of cervical (C3/C4) unilateral dorsolateral funiculotomy ablating the rubrospinal tract but sparing the dorsal and ventral corticospinal tract [79]. In this model of cervical lesion, the authors did not compare the efficacy of the hydrogel to the spinal lesion alone.

Previous studies, using natural or synthetic hydrogels such as chitosan, pHPMA, PLA-*b*-PHEMA, reported behavioral improvements when transplanted in the C2 hemilesioned cavity suggesting the potential benefits of tissue engineering material [25,26,82]. In our experiment, we used a material liquid at ambient temperature and gelling at body temperature, i.e., once the temperature is raised it solidifies into a soft hydrogel allowing to be injected through small gauge needles [116,117]. Thus, our hydrogel presents the advantage to be injected into the lesion cavities and to fill all the tortuosities of these cavities better than implantable and semi-rigid hydrogels as previously described [78]. Contrary to few PNIPAAm-*g*-PEG based hydrogels developed for spinal cord repair, which were chemically cross-linked (use of dimethacrylate as a crosslinker), our designed hydrogel relied on physical non-covalent crosslinking, offering potentially improved degradation/renal excretion features [75]. Thus, our hydrogel was not strictly degradable and, as non-degradable polymers, hydrogel calcification and prolonged inflammatory response might limit long-term axonal regeneration [4,118]. In addition, axonal regeneration is restricted to the existing pores of the hydrogel that may limit the number of regenerating processes.

Thus, even if our hydrogel has a great potential for the repair of the spinal cord, it will have to be improved to make it degradable and absorbable.

4.5. PNIPAAm-g-PEG restores the post-activation depression of the H-reflex

In mammal, SCI is followed by a 'spinal shock' period characterized by a muscle paralysis, a hypotonia and a loss of reflexes below the level of injury. Several weeks after injury, these initial troubles are replaced by a spastic syndrome characterized by exaggerated tendon jerk, hypertonia and muscle spam [119]. The spinal lesion induces 1) an increase in the amplitude of the H-reflex and in the H_{max}/M_{max} ratio at the baseline stimulation and 2) a decrease in the post-activation depression upon low-frequency stimulation.

At 12 weeks post-injury, calculation of the H_{max}/M_{max} ratio at the baseline stimulation indicated that the value of the Lesion + PNIPAAM group was similar to that of the SHAM group, the value of the Lesion group remaining higher than the two other groups. Furthermore, evaluation of the rate sensitivity of the H-reflex (i.e., the decrease in reflex magnitude relative to repetition rate) indicated that animals receiving the PNIPAAm-PEG hydrogel presented, as the SHAM group, a depression when the frequency of stimulation increased. On the contrary, in the Lesion group, the H_{max}/M_{max} ratios normalized to data obtained at 0.3 Hz did not significantly decrease and remained higher than the two other groups at 5 and 10 Hz suggesting a hyper-reflexia following SCI.

Our results may suggest that the hydrogel injected into the lesion cavity may induce a beneficial reorganization of the sensori-motor loop by changing the level of sublesional motoneuron excitability. Indeed, we can hypothesize that recovery of the sensori-motor loop (and consequently of the H_{max}/M_{max} ratio) is the result of the return of the cortical and subcortical influx to networks connecting muscles from regenerating axons thought the lesion site and/or Ia afferent presynaptic inhibition and/or Ia afferent reciprocal inhibition of antagonist muscle and/or plasticity of spared descending pathways with the formation of new synapse with motoneurons or by changing the level of neurotransmitter released [120–124].

Recently, Tom et al. [115] reported a loss of frequency-dependant depression property in animals receiving PNIPAAm-*g*-PEG combined with BDNF/NT3 and no difference with SCI group. They only observed a restoration in groups in which treadmill training was added to the treatment but they did not evaluate the efficacy of the hydrogel alone. Furthermore, compared to our study, the authors used a model of moderate T9/T10 contusion injury and performed the hydrogel injection one week post-injury which could also explain the difference with our results.

In the context of spinal cord injury, biomaterial matrixes are generally used to bridge the gap created by spinal cord damage and to replace the lost tissue in order to provide support for regrowth of damaged axons. Previously, it was shown a recovery in the post-activation depression of the H-reflex after a T10 or a C2 spinal hemisection and implantation of a pHPMA or a chitosan hydrogel, respectively [25,82]. The authors concluded that the graft of a non-toxic material within the lesion cavity may bring a suitable environment for i) regenerating damaged neurons, ii) preventing the secondary damage and iii) limiting the glial scar development allowing thus a higher neuroplasticity.

Finally, no physiological reflex recovery was observed in the group of animals receiving the hydrogel when a repetitive stimulation was applied to the *Tibialis anterior* muscle in order to activate the metabosensitive (thinly myelinated and unmyelinated fibers from groups III and IV) afferent fibers. This result indicates that the hydrogel failed to restore the ascending pathways involved in ventilatory adjustments. Previously, it was showed, using pHPMA and chitosan hydrogels implanted at the T10 and C2 levels, respectively, a recovery of the adaptive ventilatory response to muscle fatigue [25,82]. The authors concluded that the implanted hydrogel allows the transmission of the sensory influxes from the muscle to the supra-spinal cord after activation of metabosensitive afferents that inform throughout the spinal pathway, the brainstem center of the muscle contraction rate. Since this recovery may have an anatomical basis, with the reorganization of segmental, intersegmental and suprasegmental nervous nertworks allowing messages to be traced back to the nervous treatment centers, our results suggest that plasticity mechanisms were not fully at play, 12 weeks post-hydrogel injection.

4.6. PNIPAAm-g-PEG supports axonal regeneration

Our results indicate that axons grew into the hydrogel and, similarly to the spared tissue, they were oriented along the rostro-caudal axis. In addition, only few glial processes colonized the hydrogel while a limited number of neurites penetrated in the glial scar. These very interesting results point out the high potential of the hydrogel to support axonal regeneration and may explain the functional recovery we observed in animals receiving copolymer, immediately after the C2 hemisection. Previously, it was reported that PNIPAAm-*g*-PEG hydrogel supported axonal regrowth when BDNF was combined to the hydrogel [78,79]. Our results are in line with these previous results and highlight the potential of the PNIPAAm-*g*-PEG copolymer for repairing the spinal cord.

4.7. The use of biomaterials in a high cervical hemisection model

The cervical hemisection interrupts descending pathways as well as propriospinal pathways to thoracic and lombosacral segments. Most of the supraspinal descending influx are conveyed to motoneurons in the ventral horn via different groups of interneurons within the intermediate grey and dorsal horn. Thus, cervical hemisection induces motor and sensory deficits in the hindlimb as well as in the forelimb and complete high cervical hemisection a functional quiescence of the ipsilateral hemidiaphragm.

Although the rat cervical hemisection model has been widely used to study different spinal cord repair strategies, few studies using biomaterials have used this model.

Thus, it was previously demonstrated, after a partial cervical hemisection completely ablating the lateral funiculus and implantation of a pHEMA or a pHEMA soaked in 1 μg of BDNF, a modest cellular inflammatory responses that disappeared by 4 weeks and minimal scarring around the hydrogel and a considerable angiogenesis promoting axonal penetration into the biomaterial [125]. In others studies in which the dorsolateral funiculus was injured at the C4 level, it was showed that, in absence of immune suppression, grafting of alginated encapsulated BDNF-producing fibroblast survived and induced by 5 weeks a partial recovery of forelimb usage in a test of vertical exploration and of hindlimb function while crossing a horizontal rope [126,127]. Immunocytochemical examination revealed RT-97, 5-HT, CGRP and GAP-43 containing axons surrounding the transplant within the lesion, indicating axonal regeneration. Furthermore, Liu et al. [128] reported, after a complete C5 lateral spinal cord hemisection, that implantation of Schwann cell-seeded alginate hydrogels combined to a caudal rAAV5-GFP/BDNF injection induced by 8 weeks a regeneration of serotoninergic (propriospinal) and descending (supraspinal) axons throughout the scaffold.

Finally, only the study of Nawrotek et al. [82] can be compared to our study. The authors studied the efficacy of a chitosan hydrogel implanted in a cervical lesion by following sensorimotor recoveries for 12 weeks and then using electrophysioogical recordings. They showed, after implantation of a chitosant hydrogel into a C2 hemisection, an improvement in the ladder climbing and grip strength test scores, in ventilatory adaptation to muscle fatigue and temporary asphyxia, and a return in the H-reflex rate sensitivity. The authors concluded that hydrogel based on chitosan constitute a promising therapeutic approach to repair damaged spinal cord. However, although chitosan is considered as a promising biocompatible biomaterial for spinal cord repair, it presents some drawbacks. Indeed, as natural biomaterials, it may contain impurities, presents poor solubility at physiological pH and a variability in its physico-chemical properties making it a biomaterial that is difficult to functionalize.

5. Conclusion

In the current study, we showed that the PNIPAAm-*g*-PEG hydrogel copolymer exhibits mandatory properties to be used as a CNS scaffold. Indeed, this hydrogel is a non toxic matrix that 1) supports survival and proliferation of hOE-MSCs *in vitro*, 2) does not increase endogenous inflammation, 3) is permissive for axonal regowth and 4) improves sensori-motor recovery. These improvements may be the result of a more suitable environment allowing axonal regeneration and survival of damaged neurons as well as limitation of the glial scar development and secondary damages and/or a higher neuroplasticity expression.

Due to its high therapeutic potential, this hydrogel is a potent candidate that can be used as an adjuvant with other strategies (rehabilitation, anti-inflammatory molecules, neurotrophic factors, stem cells …) or associated to an intravenous injectable strategy [129] to repair the spinal cord. The next step will be to optimize the copolymer by combining it with bioactive molecules and cells, in order to enhance functional outcome after SCI.

This study is part of a larger study whose goal is, ultimately, to lead to a clinical trial.

Authors' contributions

All the authors equally conceived, designed and performed the experiment, analyzed the data, performed the statistical analysis and wrote the paper. All authors read and approved the final manuscript.

Availability of data and material

All data analyzed during this study are included in this publication. The datasets during and/or analyzed during the current study are available from the corresponding author on reasonable request.

Declaration of competing interest

The authors declare that they have no known competing financial interests or personal relationships that could have appeared to influence the work reported in this paper.

Acknowledgments

This work was supported by public [*Aix-Marseille Université* (AMU) and *Centre National de la Recherche Scientifique* (CNRS)] and private [Combattre la Paralysie Association] grants.

Appendix A. Supplementary data

Supplementary data to this article can be found online at https://doi.org/10.1016/j.msec.2019.110354.

References

[1] S.W. Liu, T. Schackel, N. Weidner, R. Puttagunta, Biomaterial-supported cell transplantation treatments for spinal cord injury: challenges and perspectives, Front. Cell. Neurosci. 11 (2018).
[2] M.J. Moore, J.A. Friedman, E.B. Lewellyn, S.M. Mantila, A.J. Krych, S. Ameenuddin, et al., Multiple-channel scaffolds to promote spinal cord axon regeneration, Biomaterials 27 (2006) 419–429.
[3] D.N. Rocha, P. Brites, C. Fonseca, A.P. Pego, Poly(Trimethylene carbonate-co-epsilon-caprolactone) promotes axonal growth, PLoS One 9 (2014).
[4] K.S. Straley, C.W.P. Foo, S.C. Heilshorn, Biomaterial design strategies for the treatment of spinal cord injuries, J. Neurotrauma 27 (2010) 1–19.
[5] A.E. Haggerty, M. Oudega, Biomaterials for spinal cord repair, Neuroscience Bulletin 29 (2013) 445–459.
[6] B. Shrestha, K. Coykendall, Y.C. Li, A. Moon, P. Priyadarshani, L. Yao, Repair of injured spinal cord using biomaterial scaffolds and stem cells, Stem Cell Res. Ther. 5 (2014).
[7] N.N. Madigan, S. McMahon, T. O'Brien, M.J. Yaszemski, A.J. Windebank, Current tissue engineering and novel therapeutic approaches to axonal regeneration following spinal cord injury using polymer scaffolds, Respir. Physiol. Neurobiol. 169 (2009) 183–199.
[8] M. Tsintou, K. Dalamagkas, A.M. Seifalian, Advances in regenerative therapies for spinal cord injury: a biomaterials approach, Neural Regeneration Research 10 (2015) 726–742.
[9] W. Potter, R.E. Kalil, W.J. Kao, Biomimetic material systems for neural progenitor cell-based therapy, Frontiers in Bioscience-Landmark 13 (2008) 806–821.
[10] T. Fuhrmann, P.N. Anandakumaran, M.S. Shoichet, Combinatorial therapies after spinal cord injury: how can biomaterials help? Adv. Healthc. Mater. 6 (2017).
[11] A.M. Ziemba, R.J. Gilbert, Biomaterials for local, controlled drug delivery to the injured spinal cord, Front. Pharmacol. 8 (2017).
[12] D. Macaya, M. Spector, Injectable hydrogel materials for spinal cord regeneration: a review, Biomed. Mater. 7 (2012).
[13] O.A. Carballo-Molina, I. Velasco, Hydrogels as scaffolds and delivery systems to enhance axonal regeneration after injuries, Front. Cell. Neurosci. 9 (2015).
[14] B.V. Slaughter, S.S. Khurshid, O.Z. Fisher, A. Khademhosseini, N.A. Peppas, Hydrogels in regenerative medicine, Adv. Mater. 21 (2009) 3307–3329.
[15] G. Perale, F. Rossi, E. Sundstrom, S. Bacchiega, M. Masi, G. Forloni, et al., Hydrogels in spinal cord injury repair strategies, ACS Chem. Neurosci. 2 (2011) 336–345.
[16] D. Gupta, C.H. Tator, M.S. Shoichet, Fast-gelling injectable blend of hyaluronan and methylcellulose for intrathecal, localized delivery to the injured spinal cord, Biomaterials 27 (2006) 2370–2379.
[17] R. Censi, P. Di Martino, T. Vermonden, W.E. Hennink, Hydrogels for protein delivery in tissue engineering, J. Control. Release 161 (2012) 680–692.
[18] H.K. Kleinman, M.L. Mcgarvey, J.R. Hassell, V.L. Star, F.B. Cannon, G.W. Laurie, et al., Basement-membrane complexes with biological-activity, Biochemistry 25 (1986) 312–318.
[19] V.M. Tysseling, V. Sahni, E.T. Pashuck, D. Birch, A. Hebert, C. Czeisler, et al., Self-assembling peptide amphiphile promotes plasticity of serotonergic fibers following spinal cord injury, J. Neurosci. Res. 88 (2010) 3161–3170.
[20] A. Hejcl, J. Ruzicka, M. Kapcalova, K. Turnovcova, E. Krumbholcova, M. Pradny, et al., Adjusting the chemical and physical properties of hydrogels leads to improved stem cell survival and tissue ingrowth in spinal cord injury reconstruction: a comparative study of four methacrylate hydrogels, Stem Cells Dev. 22 (2013) 2794–2805.
[21] T.H. Kim, D.B. An, S.H. Oh, M.K. Kang, H.H. Song, J.H. Lee, Creating stiffness gradient polyvinyl alcohol hydrogel using a simple gradual freezing-thawing method to investigate stem cell differentiation behaviors, Biomaterials 40 (2015) 51–60.
[22] P.A. Ramires, M.A. Miccoli, E. Panzarini, L. Dini, C. Protopapa, In vitro and in vivo biocompatibility evaluation of a polyalkylimide hydrogel for soft tissue augmentation, J. Biomed. Mater. Res. B Appl. Biomater. 72B (2005) 230–238.
[23] C.Y. Yang, B.B. Song, Y. Ao, A.P. Nowak, R.B. Abelowitz, R.A. Korsak, et al., Biocompatibility of amphiphilic diblock copolypeptide hydrogels in the central nervous system, Biomaterials 30 (2009) 2881–2898.
[24] M.F. Rauch, S.R. Hynes, J. Bertram, A. Redmond, R. Robinson, C. Williams, et al., Engineering angiogenesis following spinal cord injury: a coculture of neural progenitor and endothelial cells in a degradable polymer implant leads to an increase in vessel density and formation of the blood-spinal cord barrier, Eur. J. Neurosci. 29 (2009) 132–145.
[25] V. Pertici, J. Amendola, J. Laurin, D. Gigmes, L. Madaschi, S. Carelli, et al., The use of poly(N-[2-hydroxypropyl]-methacrylamide) hydrogel to repair a T10 spinal cord hemisection in rat: a behavioural, electrophysiological and anatomical examination, Asn Neuro 5 (2013) 149–166.
[26] V. Pertici, T. Trimaille, J. Laurin, M.S. Felix, T. Marqueste, B. Pettmann, et al., Repair of the injured spinal cord by implantation of a synthetic degradable block copolymer in rat, Biomaterials 35 (2014) 6248–6258.
[27] V. Estrada, N. Brazda, C. Schmitz, S. Heller, H. Blazyca, R. Martini, et al., Long-lasting significant functional improvement in chronic severe spinal cord injury following scar resection and polyethylene glycol implantation, Neurobiol. Dis. 67 (2014) 165–179.
[28] S. Woerly, Hydrogels for neural tissue reconstruction and transplantation, Biomaterials 14 (1993) 1056–1058.
[29] S. Woerly, S. Fort, I. Pignot-Paintrand, C. Cottet, C. Carcenac, M. Savasta, Development of a sialic acid-containing hydrogel of poly[N-(2-hydroxypropyl) methacrylamide]: characterization and implantation study, Biomacromolecules 9 (2008) 2329–2337.
[30] H. Nomura, Y. Katayama, M.S. Shoichet, C.H. Tator, Complete spinal cord transection treated by implantation of a reinforced synthetic hydrogel channel results in syringomyelia and caudal migration of the rostral stump, Neurosurgery 59 (2006) 183–192.
[31] A. Hejcl, P. Lesny, M. Pradny, J. Michalek, P. Jendelova, J. Stulik, et al., Biocompatible hydrogels in spinal cord injury repair, Physiol. Res. 57 (2008) S121–S132.
[32] A. Hejcl, L. Urdzikova, J. Sedy, P. Lesny, M. Pradny, J. Michalek, et al., Acute and delayed implantation of positively charged 2-hydroxyethyl methacrylate scaffolds in spinal cord injury in the rat, J. Neurosurg. Spine 8 (2008) 67–73.
[33] A. Hejcl, P. Lesny, M. Pradny, J. Sedy, J. Zamecnik, P. Jendelova, et al., Macroporous hydrogels based on 2-hydroxyethyl methacrylate. Part 6: 3D hydrogels with positive and negative surface charges and polyelectrolyte complexes in spinal cord injury repair, J. Mater. Sci. Mater. Med. 20 (2009) 1571–1577.
[34] A. Hejcl, J. Sedy, M. Kapcalova, D.A. Toro, T. Amemori, P. Lesny, et al., HPMA-RGD hydrogels seeded with mesenchymal stem cells improve functional outcome in chronic spinal cord injury, Stem Cells Dev. 19 (2010) 1535–1546.
[35] L.R. Pires, A.P. Pego, Bridging the lesion-engineering a permissive substrate for nerve regeneration, Regenerative Biomaterials 2 (2015) 203–214.

[36] E.C. Tsai, P.D. Dalton, M.S. Shoichet, C.H. Tator, Synthetic hydrogel guidance channels facilitate regeneration of adult rat brainstem motor axons after complete spinal cord transection, J. Neurotrauma 21 (2004) 789–804.
[37] X.B. Kong, Q.Y. Tang, X.Y. Chen, Y. Tu, S.Z. Sun, Z.L. Sun, Polyethylene glycol as a promising synthetic material for repair of spinal cord injury, Neural Regeneration Research 12 (2017) 1003–1008.
[38] J. Luo, R. Borgens, R.Y. Shi, Polyethylene glycol improves function and reduces oxidative stress in synaptosomal preparations following spinal cord injury, J. Neurotrauma 21 (2004) 994–1007.
[39] E. Sykova, P. Jendelova, L. Urdzikova, P. Lesny, A. Hejcl, Bone marrow stem cells and polymer hydrogels-two strategies for spinal cord injury repair, Cell. Mol. Neurobiol. 26 (2006) 1113–1129.
[40] E. Sykova, P. Jendelova, In vivo tracking of stem cells in brain and spinal cord injury, Neurotrauma: New Insights into Pathology and Treatment 161 (2007) 367–383.
[41] P.D. Dalton, L. Flynn, M.S. Shoichet, Manufacture of poly(2-hydroxyethyl methacrylate-co-methyl methacrylate) hydrogel tubes for use as nerve guidance channels, Biomaterials 23 (2002) 3843–3851.
[42] S. Giannetti, L. Lauretti, E. Fernandez, F. Salvinelli, G. Tamburrini, R. Pallini, Acrylic hydrogel implants after spinal cord lesion in the adult rat, Neurol. Res. 23 (2001) 405–409.
[43] J.S. Katz, J.A. Burdick, Hydrogel mediated delivery of trophic factors for neural repair, Wiley Interdisciplinary Reviews-Nanomedicine and Nanobiotechnology 1 (2009) 128–139.
[44] M.M. Pakulska, B.G. Ballios, M.S. Shoichet, Injectable hydrogels for central nervous system therapy, Biomed. Mater. 7 (2012).
[45] J. Guo, H. Su, Y. Zeng, Y.X. Liang, W.M. Wong, R.G. Ellis-Behnke, et al., Reknitting the injured spinal cord by self-assembling peptide nanofiber scaffold, Nanomed. Nanotechnol. Biol. Med. 3 (2007) 311–321.
[46] V.M. Tysseling-Mattiace, V. Sahni, K.L. Niece, D. Birch, C. Czeisler, M.G. Fehlings, et al., Self-assembling nanofibers inhibit glial scar formation and promote axon elongation after spinal cord injury, J. Neurosci. 28 (2008) 3814–3823.
[47] Y. Liu, H. Ye, K. Satkunendrarajah, G.S. Yao, Y. Bayon, M.G. Fehlings, A self-assembling peptide reduces glial scarring, attenuates post-traumatic inflammation and promotes neurological recovery following spinal cord injury, Acta Biomater. 9 (2013) 8075–8088.
[48] J. Piantino, J.A. Burdick, D. Goldberg, R. Langer, L.I. Benowitz, An injectable, biodegradable hydrogel for trophic factor delivery enhances axonal rewiring and improves performance after spinal cord injury, Exp. Neurol. 201 (2006) 359–367.
[49] L. Klouda, A.G. Mikos, Thermoresponsive hydrogels in biomedical applications, Eur. J. Pharm. Biopharm. 68 (2008) 34–45.
[50] L.S. Yap, M.C. Yang, Evaluation of hydrogel composing of Pluronic F127 and carboxymethyl hexanoyl chitosan as injectable scaffold for tissue engineering applications, Colloids Surfaces B Biointerfaces 146 (2016) 204–211.
[51] I.M.A. Diniz, C. Chen, X.T. Xu, S. Ansari, H.H. Zadeh, M.M. Marques, et al., Pluronic F-127 hydrogel as a promising scaffold for encapsulation of dental-derived mesenchymal stem cells, J. Mater. Sci. Mater. Med. 26 (2015).
[52] S.F. Nie, W.L.W. Hsiao, W.S. Pan, Z.J. Yang, Thermoreversible Pluronic (R) F127-based hydrogel containing liposomes for the controlled delivery of paclitaxel: in vitro drug release, cell cytotoxicity, and uptake studies, Int. J. Nanomed. 6 (2011) 151–166.
[53] J.M. Barichello, M. Morishita, K. Takayama, T. Nagai, Absorption of insulin from Pluronic F-127 gels following subcutaneous administration in rats, Int. J. Pharm. 184 (1999) 189–198.
[54] M. Guzman, F.F. Garcia, J. Molpeceres, M.R. Aberturas, Polyoxyethylene-polyoxypropylene block copolymer gels as sustained-release vehicles for subcutaneous drug administration, Int. J. Pharm. 80 (1992) 119–127.
[55] Y. Yang, J.C. Wang, X. Zhang, W.L. Lu, Q. Zhang, A novel mixed micelle gel with thermo-sensitive property for the local delivery of docetaxel, J. Control. Release 135 (2009) 175–182.
[56] D.F. Liu, T. Jiang, W.H. Cai, J. Chen, H.B. Zhang, S. Hietala, et al., An in situ gelling drug delivery system for improved recovery after spinal cord injury, Adv. Healthc. Mater. 5 (2016) 1513–1521.
[57] P.Z. Elias, G.W. Liu, H. Wei, M.C. Jensen, P.J. Horner, S.H. Pun, A functionalized, injectable hydrogel for localized drug delivery with tunable thermosensitivity: synthesis and characterization of physical and toxicological properties, J. Control. Release 208 (2015) 76–84.
[58] S.S. Zhang, J.E. Burda, M.A. Anderson, Z.R. Zhao, Y. Ao, Y. Cheng, et al., Thermoresponsive copolypeptide hydrogel vehicles for central nervous system cell delivery, ACS Biomater. Sci. Eng. 1 (2015) 705–717.
[59] L. Chen, X.Q. Li, L.P. Cao, X.L. Li, J.R. Meng, J. Dong, et al., An injectable hydrogel with or without drugs for prevention of epidural scar adhesion after laminectomy in rats, Chin. J. Polym. Sci. 34 (2016) 147–163.
[60] L.T.A. Hong, Y.M. Kim, H.H. Park, D.H. Hwang, Y. Cui, E.M. Lee, et al., An injectable hydrogel enhances tissue repair after spinal cord injury by promoting extracellular matrix remodeling, Nat. Commun. 8 (2017).
[61] W.R. Kim, M.J. Kang, H. Park, H.J. Ham, H. Lee, D. Geum, Functional test scales for evaluating cell-based therapies in animal models of spinal cord injury, Stem Cell. Int. 2017 (2017) 5160261https://doi.org/10.1155/2017/5160261 12 pages.
[62] L. Klouda, K.R. Perkins, B.M. Watson, M.C. Hacker, S.J. Bryant, R.M. Raphael, et al., Thermoresponsive, in situ cross-linkable hydrogels based on N-isopropylacrylamide: fabrication, characterization and mesenchymal stem cell encapsulation, Acta Biomater. 7 (2011) 1460–1467.
[63] J. Vernengo, G.W. Fussell, N.G. Smith, A.M. Lowman, Evaluation of novel injectable hydrogels for nucleus pulposus replacement, J. Biomed. Mater. Res. B Appl. Biomater. 84B (2008) 64–69.
[64] S. Fujishige, K. Kubota, I. Ando, Phase-transition of aqueous-solutions of poly(N-isopropylacrylamide) and poly(N-isopropylmethacrylamide), J. Phys. Chem. 93 (1989) 3311–3313.
[65] E.S. Gil, S.M. Hudson, Stimuli-reponsive polymers and their bioconjugates, Prog. Polym. Sci. 29 (2004) 1173–1222.
[66] M. Ebara, M. Yamato, M. Hirose, T. Aoyagi, A. Kikuchi, K. Sakai, et al., Copolymerization of 2-carboxyisopropylacrylamide with N-isopropylacrylamide accelerates cell detachment from grafted surfaces by reducing temperature, Biomacromolecules 4 (2003) 344–349.
[67] Y. Shi, C.B. Ma, L.L. Peng, G.H. Yu, Conductive "smart" hybrid hydrogels with PNIPAM and nanostructured conductive polymers, Adv. Funct. Mater. 25 (2015) 1219–1225.
[68] Y.Y. Liu, Y.H. Shao, J. Lu, Preparation, properties and controlled release behaviors of pH-induced thermosensitive amphiphilic gels, Biomaterials 27 (2006) 4016–4024.
[69] H. Hatakeyama, A. Kikuchi, M. Yamato, T. Okano, Bio-functionalized thermo-responsive interfaces facilitating cell adhesion and proliferation, Biomaterials 27 (2006) 5069–5078.
[70] M. Nakayama, T. Okano, T. Miyazaki, F. Kohori, K. Sakai, M. Yokoyama, Molecular design of biodegradable polymeric micelles for temperature-responsive drug release, J. Control. Release 115 (2006) 46–56.
[71] D.C. Coughlan, F.P. Quilty, O.I. Corrigan, Effect of drug physicochemical properties on swelling/deswelling kinetics and pulsatile drug release from thermo-responsive poly(N-isopropylacrylamide) hydrogels, J. Control. Release 98 (2004) 97–114.
[72] K. Na, J.H. Park, S.W. Kim, B.K. Sun, D.G. Woo, H.M. Chung, et al., Delivery of dexamethasone, ascorbate, and growth factor (TGF beta-3) in thermo-reversible hydrogel constructs embedded with rabbit chondrocytes, Biomaterials 27 (2006) 5951–5957.
[73] A. Chilkoti, M.R. Dreher, D.E. Meyer, D. Raucher, Targeted drug delivery by thermally responsive polymers, Adv. Drug Deliv. Rev. 54 (2002) 613–630.
[74] X. Yin, A.S. Hoffman, P.S. Stayton, Poly(N-isopropylacrylamide-co-propylacrylic acid) copolymers that respond sharply to temperature and pH, Biomacromolecules 7 (2006) 1381–1385.
[75] A. Alexander, Ajazuddin, J. Khan, S. Saraf, S. Saraf, Polyethylene glycol (PEG)-Poly(N-isopropylacrylamide) (PNIPAAm) based thermosensitive injectable hydrogels for biomedical applications, Eur. J. Pharm. Biopharm. 88 (2014) 575–585.
[76] N. Comolli, B. Neuhuber, I. Fischer, A. Lowman, In vitro analysis of PNIPAAm-PEG, a novel, injectable scaffold for spinal cord repair, Acta Biomater. 5 (2009) 1046–1055.
[77] A.M. Akimoto, E. Hasuike, H. Tada, K. Nagase, T. Okano, H. Kanazawa, et al., Design of tetra-arm PEG-crosslinked thermoresponsive hydrogel for 3D cell culture, Anal. Sci. 32 (2016) 1203–1205.
[78] L. Conova, J. Vernengo, Y. Jin, B.T. Himes, B. Neuhuber, I. Fischer, et al., A pilot study of poly(N-isopropylacrylamide)-g-polyethylene glycol and poly(N-isopropylacrylamide)-g-methylcellulose branched copolymers as injectable scaffolds for local delivery of neurotrophins and cellular transplants into the injured spinal cord, J. Neurosurg. Spine 15 (2011) 594–604.
[79] L.C. Grous, J. Vernengo, Y. Jin, B.T. Himes, J.S. Shumsky, I. Fischer, et al., Implications of poly(N-isopropylacrylamide)-g-poly(ethylene glycol) with co-dissolved brain-derived neurotrophic factor injectable scaffold on motor function recovery rate following cervical dorsolateral funiculotomy in the rat, J. Neurosurg. Spine 18 (2013) 641–652.
[80] S.D. Girard, A. Deveze, E. Nivet, B. Gepner, F.S. Roman, F. Feron, Isolating nasal olfactory stem cells from rodents or humans, Jove-Journal of Visualized Experiments 54 (2011) 1–5 article number: e2762.
[81] Y. Gueye, T. Marqueste, F. Maurel, M. Khrestchatisky, P. Decherchi, F. Feron, Cholecalciferol (vitamin D-3) improves functional recovery when delivered during the acute phase after a spinal cord trauma, J. Steroid Biochem. Mol. Biol. 154 (2015) 23–31.
[82] K. Nawrotek, T. Marqueste, Z. Modrzejewska, R. Zarzycki, A. Rusak, P. Decherchi, Thermogelling chitosan lactate hydrogel improves functional recovery after a C2 spinal cord hemisection in rat, J. Biomed. Mater. Res. A 105 (2017) 2004–2019.
[83] H.G.J.M. Kuypers, Anatomy of Descending Pathways. Comprehensive Physiology, American Physiological Society, Washington, D.C, 1981, pp. 597–655.
[84] P.J. Harrison, H. Hultborn, E. Jankowska, R. Katz, B. Storai, D. Zytnicki, Labeling of interneurones by retrograde transsynaptic transport of horseradish-peroxidase from motoneurones in rats and cats, Neurosci. Lett. 45 (1984) 15–19.
[85] P. Decherchi, P. Gauthier, Regeneration of acutely and chronically injured descending respiratory pathways within post-traumatic nerve grafts, Neuroscience 112 (2002) 141–152.
[86] M. Martinez, J.M. Brezun, L. Bonnier, C. Xerri, A new rating scale for open-field evaluation of behavioral recovery after cervical spinal cord injury in rats, J. Neurotrauma 26 (2009) 1043–1053.
[87] Y. Li, P. Decherchi, G. Raisman, Transplantation of olfactory ensheathing cells into spinal cord lesions restores breathing and climbing, J. Neurosci. 23 (2003) 727–731.
[88] G.A. Metz, I.Q. Whishaw, Cortical and subcortical lesions impair skilled walking in the ladder rung walking test: a new task to evaluate fore- and hindlimb stepping, placing, and co-ordination, J. Neurosci. Methods 115 (2002) 169–179.
[89] K.D. Anderson, A. Gunawan, O. Steward, Quantitative assessment of forelimb motor function after cervical spinal cord injury in rats: relationship to the corticospinal tract, Exp. Neurol. 194 (2005) 161–174.
[90] E. Ezer, L. Szporny, Tape test as a simple new method for study of compounds increasing problem-solving ability of rat, Psychopharmacology 48 (1976) 97–99.
[91] N.D. Fagoe, C.L. Attwell, R. Eggers, L. Tuinenbreijer, D. Kouwenhoven,

J. Verhaagen, et al., Evaluation of five tests for sensitivity to functional deficits following cervical or thoracic dorsal column transection in the rat, PLoS One 11 (2016).
[92] J. Bianco, Y. Gueye, T. Marqueste, O. Alluin, J.J. Risso, S. Garcia, et al., Vitamin D-3 improves respiratory adjustment to fatigue and H-reflex responses in paraplegic adult rats, Neuroscience 188 (2011) 182–192.
[93] G. Caron, T. Marqueste, P. Decherchi, Restoration of post-activation depression of the H-reflex by treadmill exercise in aged rats, Neurobiol. Aging 42 (2016) 61–68.
[94] F.J. Thompson, P.J. Reier, C.C. Lucas, R. Parmer, Altered patterns of reflex excitability subsequent to contusion injury of the rat spinal-cord, J. Neurophysiol. 68 (1992) 1473–1486.
[95] R.D. Skinner, J.D. Houle, N.B. Reese, C.L. Berry, E. GarciaRill, Effects of exercise and fetal spinal cord implants on the H-reflex in chronically spinalized adult rats, Brain Res. 729 (1996) 127–131.
[96] H.J. Lee, I. Jakovcevski, N. Radonjic, L. Hoelters, M. Schachner, A. Irintchev, Better functional outcome of compression spinal cord injury in mice is associated with enhanced H-reflex responses, Exp. Neurol. 216 (2009) 365–374.
[97] J.K. Lee, G.S. Emch, C.S. Johnson, J.R. Wrathall, Effect of spinal cord injury severity on alterations of the H-reflex, Exp. Neurol. 196 (2005) 430–440.
[98] N.B. Reese, R.D. Skinner, D. Mitchell, C. Yates, C.N. Barnes, T.S. Kiser, et al., Restoration of frequency-dependent depression of the H-reflex by passive exercise in spinal rats, Spinal Cord 44 (2006) 28–34.
[99] P. Decherchi, E. Dousset, Y. Jammes, Respiratory and cardiovascular responses evoked by tibialis anterior muscle afferent fibers in rats, Exp. Brain Res. 183 (2007) 299–312.
[100] M.C. Hacker, L. Klouda, B.B. Ma, J.D. Kretlow, A.G. Mikos, Synthesis and characterization of injectable, thermally and chemically gelable, amphiphilic poly(N-isopropylacrylamide)-based macromers, Biomacromolecules 9 (2008) 1558–1570.
[101] P. Caliceti, F.M. Veronese, Pharmacokinetic and biodistribution properties of poly (ethylene glycol)-protein conjugates, Adv. Drug Deliv. Rev. 55 (2003) 1261–1277.
[102] A. Karimi, A. Shojaei, P. Tehrani, Mechanical properties of the human spinal cord under the compressive loading, J. Chem. Neuroanat. 86 (2017) 15–18.
[103] A.S. Wadajkar, B. Koppolu, M. Rahimi, K.T. Nguyen, Cytotoxic evaluation of N-isopropylacrylamide monomers and temperature-sensitive poly(N-isopropylacrylamide) nanoparticles, J. Nanoparticle Res. 11 (2009) 1375–1382.
[104] H. Vihola, A. Laukkanen, L. Valtola, H. Tenhu, J. Hirvonen, Cytotoxicity of thermosensitive polymers poly(N-isopropylacrylamide), poly(N-vinylcaprolactam) and amphiphilically modified poly(N-vinylcaprolactam), Biomaterials 26 (2005) 3055–3064.
[105] M. Tunesi, S. Chierchia, S. Rodilossi, T. Russo, A. Gloria, L. Ambrosio, et al., Development and analysis of PNIPAAM and PNIPAL/PEG hydrogels for brain neurodegeneration, in: A. Riccardo, V. Brucato, L. Rimondini, G. Spadaro (Eds.), I materiali biocompatibili per la medicina, Convegno Nazionale Biomeriali, Palermo, 2014.
[106] M. Adil, T. Gaj, A. Rao, R. Kulkarni, C. Fuentes, G. Ramadoss, et al., hESC-derived striatal cells generated in a 3D hydrogel promote recovery in a huntington's disease mouse model, Mol. Ther. 26 (2018) 33-33.
[107] M.M. Adil, T. Gaj, A.T. Rao, R.U. Kulkarni, C.M. Fuentes, G.N. Ramadoss, et al., hPSC-derived striatal cells generated using a scalable 3D hydrogel promote recovery in a Huntington disease mouse model, Stem Cell Reports 10 (2018) 1481–1491.
[108] M.M. Adil, G.M.C. Rodrigues, R.U. Kulkarni, A.T. Rao, N.E. Chernavsky, E.W. Miller, et al., Efficient generation of hPSC-derived midbrain dopaminergic neurons in a fully defined, scalable, 3D biomaterial platform, Sci. Rep. 7 (2017).
[109] M.M. Adil, T. Vazin, B. Ananthanarayanan, G.M.C. Rodrigues, A.T. Rao, R.U. Kulkarni, et al., Engineered hydrogels increase the post-transplantation survival of encapsulated hESC-derived midbrain dopaminergic neurons, Biomaterials 136 (2017) 1–11.
[110] A.K. Varma, A. Das, G. Wallace, J. Barry, A.A. Vertegel, S.K. Ray, et al., Spinal cord injury: a review of current therapy, future treatments, and basic science frontiers, Neurochem. Res. 38 (2013) 895–905.
[111] N.A. Silva, N. Sousa, R.L. Reis, A.J. Salgado, From basics to clinical: a comprehensive review on spinal cord injury, Prog. Neurobiol. 114 (2014) 25–57.
[112] C.S. Ahuja, S. Nori, L. Tetreault, J. Wilson, B. Kwon, J. Harrop, et al., Traumatic spinal cord injury-repair and regeneration, Neurosurgery 80 (2017) S9–S22.
[113] C.S. Ahuja, J.R. Wilson, S. Nori, M.R.N. Kotter, C. Druschel, A. Curt, et al., Traumatic spinal cord injury, Nature Reviews Disease Primers 3 (2017).
[114] Y.D. Teng, E.B. Lavik, X.L. Qu, K.I. Park, J. Ourednik, D. Zurakowski, et al., Functional recovery following traumatic spinal cord injury mediated by a unique polymer scaffold seeded with neural stem cells (vol 99, pg 3024, 2002), Proc. Natl. Acad. Sci. U.S.A. 99 (2002) 9606-9606.
[115] B. Tom, J. Witko, M. Lemay, A. Singh, Effects of bioengineered scaffold loaded with neurotrophins and locomotor training in restoring H-reflex responses after spinal cord injury, Exp. Brain Res. 236 (2018) 3077–3084.
[116] K.Y. Lee, D.J. Mooney, Hydrogels for tissue engineering, Chem. Rev. 101 (2001) 1869–1879.
[117] X.D. Xu, H. Wei, X.Z. Zhang, S.X. Cheng, R.X. Zhuo, Fabrication and characterization of a novel composite PNIPAAm hydrogel for controlled drug release, J. Biomed. Mater. Res. A 81A (2007) 418–426.
[118] S. Vijayasekaran, T.V. Chirila, T.A. Robertson, X. Lou, J.H. Fitton, C.R. Hicks, et al., Calcification of poly(2-hydroxyethyl methacrylate) hydrogel sponges implanted in the rabbit cornea: a 3-month study, J. Biomater. Sci. Polym. Ed. 11 (2000) 599–615.
[119] L.P. Hiersemenzel, A. Curt, V. Dietz, From spinal shock to spasticity - neuronal adaptations to a spinal cord injury, Neurology 54 (2000) 1574–1582.
[120] A. Frigon, S. Rossignol, Functional plasticity following spinal cord lesions, Reprogramming the Brain 157 (2006) 231–+.
[121] H. Hultborn, Changes in neuronal properties and spinal reflexes during development of spasticity following spinal cord lesions and stroke: studies in animal models and patients, J. Rehabil. Med. 35 (2003) 46–55.
[122] Y.R. Li, D.J. Bennett, Persistent sodium and calcium currents cause plateau potentials in motoneurons of chronic spinal rats, J. Neurophysiol. 90 (2003) 857–869.
[123] I. Engberg, A. Lundberg, R.W. Ryall, Reticulospinal inhibition of interneurons, J. Physiol. 194 (1968) 225–236.
[124] I. Engberg, A. Lundberg, R.W. Ryall, Reticulospinal inhibition of transmission in reflex pathway, J. Physiol. 194 (1968) 201–223.
[125] A. Bakshi, O. Fisher, T. Dagci, B.T. Himes, I. Fischer, A. Lowman, Mechanically engineered hydrogel scaffolds for axonal growth and angiogenesis after transplantation in spinal cord injury, J. Neurosurg. Spine 1 (2004) 322–329.
[126] C.A. Tobias, N.O. Dhoot, M.A. Wheatley, A. Tessler, M. Murray, I. Fischer, Grafting of encapsulated BDNF-producing fibroblasts into the injured spinal cord without immune suppression in adult rats, J. Neurotrauma 18 (2001) 287–301.
[127] C.A. Tobias, S.S.W. Han, J.S. Shumsky, D. Kim, M. Tumolo, N.O. Dhoot, et al., Alginate encapsulated BDNF-producing fibroblast grafts permit recovery of function after spinal cord injury in the absence of immune suppression, J. Neurotrauma 22 (2005) 138–156.
[128] S.W. Liu, B. Sandner, T. Schackel, L. Nicholson, A. Chtarto, L. Tenenbaum, et al., Regulated viral BDNF delivery in combination with Schwann cells promotes axonal regeneration through capillary alginate hydrogels after spinal cord injury, Acta Biomater. 60 (2017) 167–180.
[129] Y.L. Wang, M. Wu, L. Gu, X.L. Li, J. He, L.X. Zhou, et al., Effective improvement of the neuroprotective activity after spinal cord injury by synergistic effect of glucocorticoid with biodegradable amphipathic nanomicelles, Drug Deliv. 24 (2017) 391–401.